

Numerical Solution of the Hamilton-Jacobi-Bellman Formulation for Continuous Time Mean Variance Asset Allocation *

J. Wang † P.A. Forsyth ‡

December 20, 2008

Abstract

We solve the optimal asset allocation problem using a mean variance approach. The original mean variance optimization problem can be embedded into a class of auxiliary stochastic Linear-Quadratic (LQ) problems using the method in (Zhou and Li, 2000; Li and Ng, 2000). We use a finite difference method with fully implicit timestepping to solve the resulting non-linear Hamilton-Jacobi-Bellman (HJB) PDE, and present the solutions in terms of an efficient frontier and an optimal asset allocation strategy. The numerical scheme satisfies sufficient conditions to ensure convergence to the viscosity solution of the HJB PDE. We handle various constraints on the optimal policy. Numerical tests indicate that realistic constraints can have a dramatic effect on the optimal policy compared to the unconstrained solution.

Keywords: Optimal control, mean variance tradeoff, HJB equation, viscosity solution

JEL Classification: C63, G11

AMS Classification 65N06, 93C20

1 Introduction

Continuous time mean variance asset allocation has received considerable attention over the years (Zhou and Li, 2000; Li and Ng, 2000; Nguyen and Portrai, 2002; Leippold et al., 2004; Bielecki et al., 2005). Financial applications include hedging futures (Duffie and Richardson, 1991), insurance (Chiu and Li, 2006; Wang et al., 2007), pension asset allocation (Gerrard et al., 2004; Hojgaard and Vigna, 2007) and optimal execution of trades (Lorenz and Almgren, 2007). In its simplest formulation, an investor can choose to invest in a risk-free bond or a risky asset, and can dynamically alter the proportion of wealth invested in each asset, in order to achieve a mean variance efficient result.

*This work was supported by a grant from Tata Consultancy Services and the Natural Sciences and Engineering Research Council of Canada.

†David R. Cheriton School of Computer Science, University of Waterloo, Waterloo ON, Canada N2L 3G1 e-mail: j27wang@uwaterloo.ca

‡David R. Cheriton School of Computer Science, University of Waterloo, Waterloo ON, Canada N2L 3G1 e-mail: paforsyt@uwaterloo.ca

The continuous time mean variance problem does not lend itself easily to a dynamic programming formulation. There have been two main approaches to this problem. The original mean variance optimal control problem can be embedded into a class of auxiliary stochastic Linear-Quadratic (LQ) problems, which can then be solved in terms of dynamic programming (Zhou and Li, 2000; Li and Ng, 2000). Alternatively, Martingale techniques can be used (Bielecki et al., 2005). In the case of the LQ method, previous papers use analytic techniques to solve the nonlinear Hamilton-Jacobi-Bellman (HJB) PDE for special cases. In order to obtain analytic solutions, the authors typically make assumptions which allow for the possibility of unbounded borrowing and infinite negative wealth (bankruptcy). However, some analytic solutions have been developed for handling specific constraints: no stock shorting (Li et al., 2002) (but shorting the bond is still allowed) and the no bankruptcy case (Bielecki et al., 2005) (but again allowing for shorting the bond).

Although investment policy based on mean variance optimization has its critics, an advantage of this approach compared to power-law or exponential utility maximization is that the results can be easily interpreted in terms of an efficient frontier.

The objective of this paper is to develop a numerical method for solving the continuous time mean variance optimal asset allocation problem. We will use a fully numerical scheme based on solving the HJB equation resulting from the LQ formulation. Our scheme can easily handle any type of constraint (e.g. non-negative wealth, no shorting of stocks, margin requirements).

Although the methods developed in this paper can be applied to any asset allocation problem, such as those discussed in (Nguyen and Portrai, 2002; Bielecki et al., 2005; Chiu and Li, 2006; Wang et al., 2007) we will focus on asset allocation problems which are relevant to defined contribution pension plans as discussed in (Hojgaard and Vigna, 2007; Cairns et al., 2006). In (Hojgaard and Vigna, 2007), the objective is to determine the mean variance efficient strategy in terms of final wealth. In (Cairns et al., 2006), the pension plan model includes a stochastic salary component. In (Cairns et al., 2006), the problem was formulated in terms of maximizing the utility of the wealth-to-income ratio. Here, we consider the same model, but solve for the optimal continuous time mean variance efficient frontier. Note that by setting the contribution rate to zero, the pension plan problem reduces to the classical continuous time (multi-period) portfolio selection problem (Zhou and Li, 2000; Li and Ng, 2000; Li et al., 2002; Bielecki et al., 2005; Li and Zhou, 2006).

The main results of this paper are

- Based on the methods in (Forsyth and Labahn, 2008; Wang and Forsyth, 2008), we develop a fully implicit method for solving the nonlinear HJB PDE, which arises in the LQ formulation of the mean variance problem. Under the assumption that the HJB equation satisfies a strong comparison property, our methods are guaranteed to converge to the viscosity solution of the HJB equation. In addition, the policy iteration scheme used to solve the nonlinear algebraic equations at each timestep is globally convergent. Note that an explicit method would have timestep restrictions due to stability considerations. In the case of an unbounded control, the maximum stable timestep would be difficult to estimate. This problem does not arise if an implicit method is used.
- By solving the HJB PDE and a related linear PDE, we develop a numerical method for constructing the mean variance efficient frontier (in continuous time). Any type of constraint can be applied to the investment policy.

- We pay particular attention to handling various constraints on the optimal policy. In particular, in order to compare the numerical solution with the known analytic solution in special cases, it is necessary to allow for negative wealth and unbounded controls. This requires careful attention to the grid construction and form of the control as the mesh and timesteps shrink to zero.
- From a practical point of view, we observe that the addition of realistic constraints can completely alter some of the properties of the mean variance solution compared to the unconstrained control case (Li and Zhou, 2006).

We should point out here that the optimal mean variance strategy in (Zhou and Li, 2000; Li and Ng, 2000; Nguyen and Portrai, 2002; Leippold et al., 2004; Bielecki et al., 2005; Chiu and Li, 2006; Wang et al., 2007; Hojgaard and Vigna, 2007) is the *pre-commitment* strategy, i.e. once the initial strategy has been determined (as a function of the state variables) at the initial time, the investor commits to this strategy, even if the the mean variance policy, computed at a later time would differ from the pre-commitment strategy. This contrasts with the *time-consistent* policy whereby the investor optimizes the mean variance tradeoff at each instant in time, assuming optimal mean variance strategies at each later instant. The subtle distinction between these two approaches is discussed in (Basak and Chabakauri, 2007). We note that the efficient frontier for the pre-commitment strategy must always lie above the efficient frontier for the time-consistent strategy. However, there is some economic controversy about the meaning of these two approaches. We will focus on the pre-commitment policy in this paper, leaving the time-consistent problem for future work.

2 Mean Variance Efficient Wealth Case

We first consider the problem of determining the mean variance efficient strategy in terms of the investor's final wealth. We will refer to this problem in the following as the *wealth* case. This will allow an explanation of the basic approach for construction of the efficient frontier, without undue algebraic complication. For certain special cases, there are also some analytic solutions available (Hojgaard and Vigna, 2007) for this problem. This will enable us to compare with the numerical solution.

Suppose there are two assets in the market: one is risk free (e.g. a government bond) and the other is risky (e.g. a stock index). The risky asset S follows the stochastic process

$$dS = (r + \xi_1 \sigma_1)S dt + \sigma_1 S dZ_1 , \quad (2.1)$$

where dZ_1 is the increment of a Wiener process, σ_1 is volatility, r is the interest rate, ξ_1 is the market price of risk (or Sharpe ratio) and the stock drift rate can then be defined as $\mu_S = r + \xi_1 \sigma_1$. Suppose that the plan member continuously pays into the pension plan at a constant contribution rate π in the unit time. Let $W(t)$ denote the wealth accumulated in the pension plan at time t , let p denote the proportion of this wealth invested in the risky asset S , and let $(1 - p)$ denote the fraction of wealth invested in the risk free asset. Then,

$$\begin{aligned} dW &= [(r + p\xi_1 \sigma_1)W + \pi]dt + p\sigma_1 W dZ_1 , \\ W(t=0) &= \hat{w}_0 \geq 0 . \end{aligned} \quad (2.2)$$

We will use the following notation throughout this paper,

$$\begin{aligned}
E[\cdot] &: \text{ expectation operator,} \\
Var[\cdot] &: \text{ variance operator,} \\
Std[\cdot] &: \text{ standard deviation operator,} \\
E^t[\cdot], Var^t[\cdot] \text{ or } Std^t[\cdot] &: E[\cdot], Var[\cdot] \text{ or } Std[\cdot] \text{ when sitting at time } t, \\
E_p^t[\cdot], Var_p^t[\cdot] \text{ or } Std_p^t[\cdot] &: E[\cdot|p], Var[\cdot|p] \text{ or } Std[\cdot|p] \text{ when sitting at time } t.
\end{aligned} \tag{2.3}$$

Let $W_T = W(t = T)$. Given a risk level (defined as the variance of terminal wealth $Var^{t=0}[W_T]$), an investor desires her expected terminal wealth $E^{t=0}[W_T]$ to be as large as possible. Equivalently, given an expected terminal wealth $E^{t=0}[X_T]$, she wishes the risk $Var^{t=0}[W_T]$ to be as small as possible. Using a Lagrange multiplier, the control problem is then to determine the control $p(t, W(t) = w)$, where $W(t)$ is the path of W given the control $p(t, w)$, such that $p(t, w)$ maximizes

$$\max_{p(t,w)} (E^{t=0}[W_T] - \lambda Var^{t=0}[W_T]), \tag{2.4}$$

subject to stochastic process (2.2), and where $\lambda > 0$ is a given Lagrange multiplier. The multiplier λ can be interpreted as a coefficient of risk aversion. Varying $\lambda \in [0, \infty)$ allows us to draw an efficient frontier. Note we have emphasized here that the expectations in equation (2.4) are as seen at $t = 0$ (the pre-commitment solution).

We would like to use dynamic programming to determine the efficient frontier, given by equation (2.4). However, the presence of the variance term causes some difficulty. This can be avoided with the help of the following result (Zhou and Li, 2000; Li and Ng, 2000).

Theorem 2.1 *If $p^*(t, w)$ is the optimal control of problem (2.4), then $p^*(t, w)$ is also the optimal control of problem,*

$$\max_{p(t,w)} E^{t=0}[\mu W_T - \lambda W_T^2] \tag{2.5}$$

where

$$\mu = 1 + 2\lambda E_{p^*}^{t=0}[W_T]. \tag{2.6}$$

Proof. See (Zhou and Li, 2000; Li and Ng, 2000). □

2.1 Reduction to an LQ Problem

Let,

$$\begin{aligned}
\mathbb{D} &:= \text{ the set of all admissible wealth } W(t), \text{ for } 0 \leq t \leq T; \\
\mathbb{P} &:= \text{ the set of all admissible controls } p(t, w), \text{ for } 0 \leq t \leq T \text{ and } w \in \mathbb{D}.
\end{aligned} \tag{2.7}$$

Let $\gamma = \frac{\mu}{\lambda}$, then from equation (2.6),

$$\gamma = \frac{1}{\lambda} + 2E_{p^*}^{t=0}[W_T]. \tag{2.8}$$

For a fixed γ , with $\lambda > 0$, equation (2.5) is equivalent to

$$\min_{p(t,w)} E^{t=0}[(W_T - \frac{\gamma}{2})^2] . \quad (2.9)$$

Let $J(t, w, p) = E[(W_T - \frac{\gamma}{2})^2 | W(t) = w]$, where $W(t)$ is the path of W given the asset allocation strategy $p = p(t, w)$. We define

$$V(w, \tau) = \inf_{p \in \mathbb{P}} E[(W_T - \frac{\gamma}{2})^2 | W(t = T - \tau) = w] = \inf_{p \in \mathbb{P}} J(t = T - \tau, w, p) . \quad (2.10)$$

where $\tau = T - t$. Then using equation (2.2) and Ito's Lemma, we have that $V(w, \tau)$ satisfies the HJB equation

$$V_\tau = \inf_{p \in \mathbb{P}} \{ \mu_w^p V_w + \frac{1}{2} (\sigma_w^p)^2 V_{ww} \} ; \quad w \in \mathbb{D}, \quad (2.11)$$

with terminal condition

$$V(w, \tau = 0) = (w - \frac{\gamma}{2})^2 , \quad (2.12)$$

and where

$$\begin{aligned} \mu_w^p &= \pi + w(r + p\sigma_1\xi_1) \\ (\sigma_w^p)^2 &= (p\sigma_1 w)^2 . \end{aligned} \quad (2.13)$$

In order to trace out the efficient frontier solution of problem (2.4), we proceed in the following way. Pick an arbitrary value of γ and solve problem (2.5), which determines the optimal control $p^*(t, w)$. We also need to determine $E_{p^*}^{t=0}[W_T]$.

Let $U = U(w, \tau) = E[W_T | W(t = T - \tau) = w, p(t = T - \tau, w) = p^*(t = T - \tau, w)]$. Then U is given from the solution to

$$U_\tau = \{ \mu_w^p U_w + \frac{1}{2} (\sigma_w^p)^2 U_{ww} \}_{p(t=T-\tau,w)=p^*(t=T-\tau,w)} ; \quad w \in \mathbb{D} , \quad (2.14)$$

with the payoff

$$U(w, \tau = 0) = w . \quad (2.15)$$

Since the most costly part of the solution of equation (2.11) is the determination of the optimal control p^* , solution of equation (2.14) is very inexpensive, since p^* is known.

Note that $E_{p^*}^{t=0}[const.] = const..$ Assume that $W = \hat{w}_0$ at $t = 0$. Then

$$\begin{aligned} V(\hat{w}_0, \tau = T) &= E_{p^*}^{t=0}[W_T^2] - \gamma E_{p^*}^{t=0}[W_T] + \frac{\gamma^2}{4} , \\ U(\hat{w}_0, \tau = T) &= E_{p^*}^{t=0}[W_T] . \end{aligned} \quad (2.16)$$

Assuming $V(\hat{w}_0, \tau = 0), U(\hat{w}_0, \tau = 0)$ are known, then for a given γ , we can then compute the pair $(Var_{p^*}^{t=0}[W_T], E_{p^*}^{t=0}[W_T])$ from $Var_{p^*}^{t=0}[W_T] = E_{p^*}^{t=0}[W_T^2] - (E_{p^*}^{t=0}[W_T])^2$.

From equation (2.8) we have that

$$\frac{1}{2\lambda} = \frac{\gamma}{2} - E_{p^*}^{t=0}[W_T] , \quad (2.17)$$

which then determines the value of λ in problem (2.4). In other words, we have determined the pair $(\text{Std}_{p^*}^{t=0}[W_T], E_{p^*}^{t=0}[W_T])$ for the optimal control p^* which solves problem (2.4), with the value of λ given from equation (2.17).

We then pick another value of γ , and obtain another point on the efficient frontier for another value of λ , and so on. Note that we are effectively using the parameter γ to trace out the efficient frontier. Since $\lambda > 0$, we must have (from equation (2.17))

$$\frac{\gamma}{2} - E_{p^*}^{t=0}[W_T] > 0 \quad (2.18)$$

for a valid point on the frontier.

Remark 2.1 *Note that the set of solutions for the original problem (2.4) is a subset of the set of controls for the auxiliary problem (2.5). As a result, the pair $(\text{Std}_{p^*}^{t=0}[W_T], E_{p^*}^{t=0}[W_T])$ from the optimal strategy of problem (2.5) may not be a point on the efficient frontier for problem (2.4). To find the efficient frontier for the original optimization problem (2.4), we construct an upper convex hull from the candidate points $(\text{Std}_{p^*}^{t=0}[W_T], E_{p^*}^{t=0}[W_T])$ obtained by varying γ .*

Remark 2.2 *If we allow an unbounded control set $\mathbb{P} = (-\infty, +\infty)$, then the total wealth can become negative (i.e. bankruptcy is allowed). In this case $\mathbb{D} = (-\infty, +\infty)$. If the control set \mathbb{P} is bounded, i.e. $\mathbb{P} = [p_{\min}, p_{\max}]$, then negative wealth is not possible, in which case $\mathbb{D} = [0, +\infty)$. We can also have $p_{\max} \rightarrow +\infty$, but prohibit negative wealth, in which case $\mathbb{D} = [0, +\infty)$ as well.*

2.2 Localization

Let,

$$\hat{\mathbb{D}} := \text{a finite computational domain which approximates the set } \mathbb{D}. \quad (2.19)$$

In order to solve the PDEs (2.11), (2.14) we need to use a finite computational domain, $\hat{\mathbb{D}} = [w_{\min}, w_{\max}]$. When $w \rightarrow \pm\infty$, we assume that

$$\begin{aligned} V(w \rightarrow \pm\infty, \tau) &\simeq H_1(\tau)w^2 + H_2(\tau)w + H_3(\tau) , \\ U(w \rightarrow \pm\infty, \tau) &\simeq J_1(\tau)w + J_2(\tau) . \end{aligned} \quad (2.20)$$

Then, taking into account the initial conditions (2.12), (2.15),

$$\begin{aligned} V(w \rightarrow \pm\infty, \tau) &\simeq e^{(2k_1+k_2)\tau}w^2 , \\ U(w \rightarrow \pm\infty, \tau) &\simeq e^{k_1\tau}w , \end{aligned} \quad (2.21)$$

where $k_1 = r + p\sigma_1\xi_1$ and $k_2 = (p\sigma_1)^2$. We consider three cases.

2.2.1 Allowing Bankruptcy, Unbounded Controls

In this case, we assume there are no constraints on $W(t)$ or on the control p , i.e., $\mathbb{D} = (-\infty, +\infty)$ and $\mathbb{P} = (-\infty, +\infty)$. Since $W(t) = w$ can be negative, bankruptcy is allowed. We call this case the *allowing bankruptcy* case.

Our numerical problem uses

$$\hat{\mathbb{D}} = [w_{\min}, w_{\max}] , \quad (2.22)$$

where $\hat{\mathbb{D}} = [w_{\min}, w_{\max}]$ is an approximation to the original set $\mathbb{D} = (-\infty, +\infty)$.

As far as the Dirichlet conditions at $w = w_{\min}, w_{\max}$, we can use the asymptotic form of the exact solution (see Section 2.3) to note that

$$p^*(t, w \rightarrow \pm\infty) \simeq -\frac{\xi_1}{\sigma_1} . \quad (2.23)$$

At $w = w_{\min}, w_{\max}$ we apply the Dirichlet conditions (2.21) with $p = p^*$ from equation (2.23).

These artificial boundary conditions will cause some error. However, we can make these errors small by choosing large values for $(|w_{\min}|, w_{\max})$. We will verify this in some subsequent numerical tests. If asymptotic forms of the solution are unavailable, we can use any reasonable estimate for p^* for $|w|$ large, and the error will be small if $(|w_{\min}|, w_{\max})$ are sufficiently large (Barles et al., 1995).

2.2.2 No Bankruptcy, No Short Sales

In this case, we assume that bankruptcy is prohibited and the investor cannot short the stock index, i.e., $\mathbb{D} = [0, +\infty)$ and $\mathbb{P} = [0, +\infty)$. We call this case the *no bankruptcy* (or *bankruptcy prohibition*) case.

Our numerical problem uses,

$$\hat{\mathbb{D}} = [0, w_{\max}] . \quad (2.24)$$

We make the assumption that $p^*(t, w_{\max}) \simeq 0$ (i.e. once the investor's wealth is very large, she prefers the riskless asset). The boundary conditions for V, U at $w = w_{\max}$ are given by equations (2.21) with $p = 0, w = w_{\max}$. We prohibit the possibility of bankruptcy ($W(t) < 0$) by requiring that (see Remark 2.3) $\lim_{w \rightarrow 0}(pw) = 0$, so that equations (2.11), (2.14) reduce to (at $w = 0$)

$$\begin{aligned} V_\tau(0, \tau) &= \pi V_w , \\ U_\tau(0, \tau) &= \pi U_w . \end{aligned} \quad (2.25)$$

2.2.3 No Bankruptcy, Bounded Control

This is a realistic case, in which we assume that bankruptcy is prohibited and infinite borrowing is not allowed. As a result, $\mathbb{D} = [0, +\infty)$ and $\mathbb{P} = [0, p_{\max}]$. We call this case the *bounded control* case.

Our numerical problem uses,

$$\hat{\mathbb{D}} = [0, w_{\max}] , \quad (2.26)$$

where w_{\max} is an approximation to the infinity boundary. Other assumptions and the boundary conditions for V and U are the same as those of no bankruptcy case introduced in Section 2.2.2.

We summarize the various cases in Table 1

Case	$\hat{\mathbb{D}}$	\mathbb{P}
Bankruptcy	$[w_{\min}, w_{\max}]$	$(-\infty, +\infty)$
No Bankruptcy	$[0, w_{\max}]$	$[0, +\infty)$
Bounded Control	$[0, w_{\max}]$	$[0, p_{\max}]$

TABLE 1: *Summary of cases.*

2.3 Analytic Solution: Unconstrained Control

Suppose that the control $p(t, w)$ is unbounded, i.e. $\mathbb{P} = (-\infty, +\infty)$. This allows infinite shorting of the risky asset and the bond. This also allows for bankruptcy, which means that $\mathbb{D} = (-\infty, +\infty)$. This is the case of *allowing bankruptcy* introduced in Section 2.2.1.

The analytic solution to this problem is given in (Hojgaard and Vigna, 2007),

$$\begin{cases} \text{Var}^{t=0}[W_T] = \frac{e^{\xi_1^2 T} - 1}{4\lambda^2} \\ E^{t=0}[W_T] = \hat{w}_0 e^{rT} + \pi \frac{e^{rT} - 1}{r} + \sqrt{e^{\xi_1^2 T} - 1} \text{Std}(W_T), \end{cases} \quad (2.27)$$

and the optimal control at any time $t \in [0, T]$ is

$$p^*(t, w) = -\frac{\xi_1}{\sigma_1 w} \left[w - (\hat{w}_0 e^{rt} + \frac{\pi}{r}(e^{rt} - 1)) - \frac{e^{-r(T-t) + \xi_1^2 T}}{2\lambda} \right]. \quad (2.28)$$

Note that when $|w| \rightarrow 0$, from equation (2.28), $p^*(t, w)w$ is a positive finite number, and that $|p^*(t, w)| \rightarrow \infty$ as $|w| \rightarrow 0$.

We can then see directly from the SDE (2.2), that $W(t)$ can be negative in this case. Hence, $\mathbb{D} = (-\infty, +\infty)$. From equation (2.28), when w is negative, $p^*(t, w)$ is negative. As a result, $p^*(t, w)w$ is positive, i.e., the total monetary amount invested in stock is still positive (the investor is long stock).

The efficient frontier $(\text{Std}_{p^*}^{t=0}[W_T], E_{p^*}^{t=0}[W_T])$ in this case is a straight line. We will use this analytic result to check our numerical solution.

Remark 2.3 *It is important to know the behaviour of p^*w as $w \rightarrow 0$, since it helps us determine whether negative wealth is admissible or not. As shown above, negative wealth is admissible for the case of allowing bankruptcy. In the case of no bankruptcy, although $p \in \mathbb{P} = [0, +\infty)$, we must have $\lim_{w \rightarrow 0}(pw) = 0$ so that $W(t) \geq 0$ for all $0 \leq t \leq T$. In particular, we need to make sure that the optimal strategy never generates negative wealth, i.e., $\text{Probability}(W(t) < 0 | p^*) = 0$ for all $0 \leq t \leq T$. We will see from the numerical solutions that boundary condition (2.25) does in fact result in $\lim_{w \rightarrow 0}(p^*w) = 0$. Hence, negative wealth is not admissible under the optimal strategy. More discussions of this issue are given in Section 6. For the bounded control case, the control is finite, thus $\lim_{w \rightarrow 0}(pw) = 0$ and negative wealth is not admissible.*

2.4 Special Case: Reduction to the Classic Multi-period Portfolio Selection Problem

The classic multi-period portfolio selection problem can be stated as the following: given some investment choices (assets) in the market, an investor seeks an optimal asset allocation strategy

over a period T with an initial wealth \hat{w}_0 . This problem has been widely studied (Merton, 1971; Zhou and Li, 2000; Li and Ng, 2000; Li et al., 2002; Bielecki et al., 2005; Li and Zhou, 2006). If we use the mean variance approach to solve this problem, then the best strategy $p^*(w, t)$ can be defined as a solution of problem (2.4). We still assume there is one risk free bond and one risky asset in the market. In this case,

$$\begin{aligned} dW &= (r + p\xi_1\sigma_1)W dt + p\sigma_1 W dZ_1 , \\ W(t=0) &= \hat{w}_0 > 0 . \end{aligned} \tag{2.29}$$

Clearly, the pension plan problem we introduced previously can be reduced to the classic multi-period portfolio selection problem by simply setting the contribution rate $\pi = 0$. All equations and boundary conditions stay the same.

The authors of (Bielecki et al., 2005) study the case with bankruptcy prohibition, i.e., $W(t)$ is forced to be nonnegative for all $t \in [0, T]$. In this case, $\mathbb{D} = [0, +\infty)$ and $\mathbb{P} = [0, +\infty)$. An analytic solution for this case is given in (Bielecki et al., 2005). Note that the stochastic control used in (Bielecki et al., 2005) is not the proportion of the total wealth invested in the stock, but the monetary amount invested in the stock. The authors of (Bielecki et al., 2005) point out that their strategy cannot be expressed as a proportional strategy. However, we will see later in Section 6 that the efficient frontier given by our approach (using the proportion as the control) converges to the analytic solution given in (Bielecki et al., 2005) (using the monetary amount as the control).

3 Wealth-to-income Ratio Case

In the previous section, we considered the expected value and variance of the terminal wealth in order to construct an efficient frontier. Many studies have shown that a desirable feature of a pension plan is that the holder's wealth W is large compared to her annual salary Y the year before she retires. In this section, instead of the terminal wealth, we determine the mean variance efficient strategy in terms of the terminal wealth-to-income ratio $X = \frac{W}{Y}$. In the following, we give a brief overview of the model developed in (Cairns et al., 2006). We still assume there are two underlying assets in the pension plan: one is risk free and the other is risky. Recall from equation (2.1) that the risky asset S follows the Geometric Brownian Motion,

$$dS = (r + \xi_1\sigma_1)S dt + \sigma_1 S dZ_1 . \tag{3.1}$$

Suppose that the plan member continuously pays into the pension plan at a fraction π of her yearly salary Y , which follows the process

$$dY = (r + \mu_Y)Y dt + \sigma_{Y_0}Y dZ_0 + \sigma_{Y_1}Y dZ_1 , \tag{3.2}$$

where μ_Y , σ_{Y_0} and σ_{Y_1} are constants, and dZ_0 is another increment of a Wiener process, which is independent of dZ_1 . Let p denote the proportion of this wealth invested in the risky asset S , and let $1 - p$ denote the fraction of wealth invested in the risk-free asset. Then

$$\begin{aligned} dW &= (r + p\xi_1\sigma_1)W dt + p\sigma_1 W dZ_1 + \pi Y dt , \\ W(t=0) &= \hat{w}_0 \geq 0 . \end{aligned} \tag{3.3}$$

Define a new state variable $X(t) = W(t)/Y(t)$, then by Ito's Lemma, we obtain

$$\begin{aligned} dX &= [\pi + X(-\mu_Y + p\sigma_1(\xi_1 - \sigma_{Y_1}) + \sigma_{Y_0}^2 + \sigma_{Y_1}^2)]dt \\ &\quad - \sigma_{Y_0}X dZ_0 + X(p\sigma_1 - \sigma_{Y_1})dZ_1, \\ X(t=0) &= \hat{x}_0 \geq 0. \end{aligned} \quad (3.4)$$

The control problem is then to determine the control $p(t, X(t) = x)$ such that $p(t, x)$ maximizes

$$\max_{p(t,x)} (E^{t=0}[X_T] - \lambda Var^{t=0}[X_T]), \quad (3.5)$$

subject to stochastic process (3.4). Similar to problem (2.4), we can use Theorem 2.1 to embed problem (3.5) into the following LQ stochastic optimal control problem

$$\begin{aligned} \max_{p(t,x)} E^{t=0}[\mu X_T - \lambda X_T^2], \\ \mu = 1 + 2\lambda E_{p^*}^{t=0}[X_T], \end{aligned} \quad (3.6)$$

where p^* is the optimal control. We still use \mathbb{D} and \mathbb{P} as the sets of all admissible wealth-to-income ratio and control. As before, we let $\hat{\mathbb{D}}$ be the localized computational domain.

Again, let $\gamma = \frac{\mu}{\lambda}$, then for a fixed γ , equation (2.5) is equivalent to

$$\min_{p(t,x)} E^{t=0}[(X_T - \frac{\gamma}{2})^2]. \quad (3.7)$$

Let $J(t, x, p) = E[(X_T - \frac{\gamma}{2})^2 | X(t) = x]$, where $X(t)$ is the path of X given the asset allocation strategy $p = p(t, x)$. We define

$$V(x, \tau) = \inf_{p \in \mathbb{P}} E[(X_T - \frac{\gamma}{2})^2 | X(t = T - \tau) = x] = \inf_{p \in \mathbb{P}} J(t = T - \tau, x, p). \quad (3.8)$$

where $\tau = T - t$. Then $V(x, \tau)$ satisfies the HJB equation

$$V_\tau = \inf_{p \in \mathbb{P}} \{ \mu_x^p V_x + \frac{1}{2} (\sigma_x^p)^2 V_{xx} \}; \quad x \in [0, +\infty), \quad (3.9)$$

with terminal condition

$$V(x, \tau = 0) = (x - \frac{\gamma}{2})^2, \quad (3.10)$$

and where

$$\begin{aligned} \mu_x^p &= \pi + x(-\mu_Y + p\sigma_1(\xi_1 - \sigma_{Y_1}) + \sigma_{Y_0}^2 + \sigma_{Y_1}^2) \\ (\sigma_x^p)^2 &= x^2(\sigma_{Y_0}^2 + (p\sigma_1 - \sigma_{Y_1})^2). \end{aligned} \quad (3.11)$$

We also solve for $U(x, \tau) = E[X_T | X(t = T - \tau) = x, p(t = T - \tau, x) = p^*(t = T - \tau, x)]$ using

$$U_\tau = \{ \mu_x^p U_x + \frac{1}{2} (\sigma_x^p)^2 U_{xx} \}_{p(t=T-\tau,x)=p^*(t=T-\tau,x)}; \quad x \in [0, +\infty), \quad (3.12)$$

with terminal condition

$$U(x, \tau = 0) = x . \quad (3.13)$$

We can then use the method described in Section 2.1 to trace out the efficient frontier solution of problem (3.5).

We consider the cases: allowing bankruptcy ($\mathbb{D} = (-\infty, +\infty)$, $\mathbb{P} = (-\infty, +\infty)$), no bankruptcy ($\mathbb{D} = [0, +\infty)$, $\mathbb{P} = [0, +\infty)$), and bounded control ($\mathbb{D} = [0, +\infty)$, $\mathbb{P} = [0, p_{\max}]$). For computational purposes, we localize the problem to $\hat{\mathbb{D}} = [x_{\min}, x_{\max}]$, and apply boundary conditions as in Section 2.2. More precisely, if $x = 0$ is a boundary, with $X < 0$ prohibited, then $\lim_{w \rightarrow 0}(px) = 0$, and hence

$$\begin{aligned} V_\tau(0, \tau) &= \pi V_x , \\ U_\tau(0, \tau) &= \pi U_x . \end{aligned} \quad (3.14)$$

The boundary conditions at $x \rightarrow \pm\infty$ are given in equation (2.21), but using x instead of w with $k_1 = -\mu_Y + p\sigma_1(\xi_1 - \sigma_{Y_1}) + \sigma_{Y_0}^2 + \sigma_{Y_1}^2$ and $k_2 = \sigma_{Y_0}^2 + (p\sigma_1 - \sigma_{Y_1})^2$.

Remark 3.1 *Although the pension plan account contains the risk free bond, the stochastic process for dX does not contain the risk free rate r . As a result, there is no risk free rate r in the HJB PDE (3.9). The drift rate (mean growth rate) for the yearly salary Y is $r + \mu_y$ in equation (3.2). If Y grows faster than the risk free rate, then $\mu_y > 0$; otherwise $\mu_y \leq 0$. Normally, we assume that the salary Y grows at the risk free rate, so $\mu_y = 0$.*

Remark 3.2 *The problem described in Section 2 can be seen as a special case of the problem described in this section. We can simply set the salary Y to be a constant (let $\sigma_{Y_0} = \sigma_{Y_1} = 0$ and $\mu_y = -r$), then $X(t)$ is reduced to $W(t)$ and PDE (3.9) is reduced to PDE (2.11).*

4 Discretization of the HJB PDE

In (Forsyth and Labahn, 2008; Wang and Forsyth, 2008), the authors develop a general framework to solve HJB PDEs in finance. We can directly apply the numerical scheme introduced in (Wang and Forsyth, 2008) to solve equations (2.11), (2.14), (3.9) and (3.12). Set

$$\mathcal{L}^p V \equiv a(z, p)V_{zz} + b(z, p)V_z , \quad (4.1)$$

where

$$z = w \ ; \ a(z, p) = \mu_w^p \ ; \ b(z, p) = \frac{1}{2}(\sigma_w^p)^2 \quad (4.2)$$

(see equation (2.13)) for the wealth case introduced in Section 2; and

$$z = x \ ; \ a(z, p) = \mu_x^p \ ; \ b(z, p) = \frac{1}{2}(\sigma_x^p)^2 \quad (4.3)$$

(see equation (3.11)) for the wealth-to-income ratio case introduced in Section 3. Then,

$$V_\tau = \inf_{p \in \mathbb{P}} \{ \mathcal{L}^p V \} , \quad (4.4)$$

and

$$U_\tau = \{ \mathcal{L}^p U \}_{p=P^*} . \quad (4.5)$$

Define a grid $\{z_0, z_1, \dots, z_q\}$ with $z_0 = z_{\min}$, $z_q = z_{\max}$ and let V_i^n be a discrete approximation to $V(z_i, \tau^n)$. Set $P^n = [p_0^n, p_1^n, \dots, p_q^n]'$, with each p_i^n a local optimal control at (z_i, τ^n) . Let $P^* = \{P^0, P^1, \dots, P^N\}$, where $\tau^N = T$. In other words, P^* contains the discrete optimal controls for all (i, n) . Let $V^n = [V_0^n, \dots, V_q^n]'$, and let $(\mathcal{L}_h^{P^n} V^n)_i$ denote the discrete form of the differential operator (4.1) at node (z_i, τ^n) . The operator (4.1) can be discretized using forward, backward or central differencing in the z direction to give

$$(\mathcal{L}_h^{P^{n+1}} V^{n+1})_i = \alpha_i^{n+1} V_{i-1}^{n+1} + \beta_i^{n+1} V_{i+1}^{n+1} - (\alpha_i^{n+1} + \beta_i^{n+1}) V_i^{n+1} . \quad (4.6)$$

Here α_i , β_i are defined in Appendix A.

Equation (4.4) can now be discretized using fully implicit timestepping along with the discretization (4.6) to give

$$\frac{V_i^{n+1} - V_i^n}{\Delta\tau} = \inf_{P^{n+1} \in \hat{P}} \left\{ (\mathcal{L}_h^{P^{n+1}} V^{n+1})_i \right\} , \quad (4.7)$$

where $\hat{P} = \{[p_0, p_1, \dots, p_q]' \mid p_i \in \mathbb{P}, 0 \leq i \leq q\}$. With P^{n+1} given from equation (4.7), then equation (4.5) can be discretized as

$$\frac{U_i^{n+1} - U_i^n}{\Delta\tau} = \left\{ (\mathcal{L}_h^{P^{n+1}} U^{n+1})_i \right\} . \quad (4.8)$$

Note that $\alpha_i^{n+1} = \alpha_i^{n+1}(p_i^{n+1})$ and $\beta_i^{n+1} = \beta_i^{n+1}(p_i^{n+1})$, that is, the discrete equation coefficients are functions of the local optimal control p_i^{n+1} . This makes equations (4.7) highly nonlinear in general.

Remark 4.1 *As mentioned in Remark 2.2, for the wealth case with allowing bankruptcy, we have $\mathbb{D} = (-\infty, +\infty)$ and $\mathbb{P} = (-\infty, +\infty)$. In this case, our W grid contains*

$$\begin{aligned} & [w_{\min}, \dots, w_{-2}, w_{-1}, w_1, w_2, \dots, w_{\max}] \\ & w_{\min} < \dots < w_{-2} < w_{-1} < 0 < w_1 < w_2 < \dots < w_{\max} \end{aligned} \quad (4.9)$$

with large $|w_{\min}|$ and w_{\max} . Note that our W grid does not contain the node $w = 0$, because if $w = 0$ is in the grid, no information can be passed between the negative value nodes and positive value nodes. We set $|w_{-1}|$ and w_1 to be small values close to zero. As Figure 1 shows, when the W grid is refined, a new node is inserted in between each two consecutive nodes, except for the pair w_{-1} and w_1 . Since $w = 0$ cannot be in the grid, we add two nodes of $w_{-1}^{new} = \frac{w_{-1}}{2}$ and $w_1^{new} = \frac{w_1}{2}$ into the grid.

Note that we could avoid this problem (near $w = 0$) by defining the control to be (pw) instead of p . However, in the more realistic case of bounded p , it is more natural to impose constraints on p , rather than on (pw) , hence we prefer to formulate the control (and constraints) in terms of the variable p .

Remark 4.2 We use a fully implicit method to solve equation (4.7). Since $p \rightarrow \infty$ in some cases, it would be a challenging task to determine the maximum stable timestep for an explicit method.

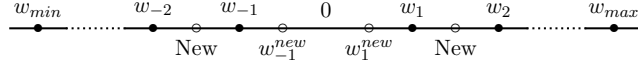


FIGURE 1: Node insertion in W grid.

4.1 Positive Coefficient Method

It is important that central, forward or backward discretizations are used to ensure that (4.7) and (4.8) are a positive coefficient discretizations. To be more precise, this condition is

Condition 4.1 *Positive Coefficient Condition*

$$\alpha_i^{n+1} \geq 0, \quad \beta_i^{n+1} \geq 0, \quad i = 0, \dots, q-1 \quad . \quad (4.10)$$

In (Wang and Forsyth, 2008), the authors develop a positive coefficient scheme for HJB PDEs in finance, which uses central differencing as much as possible. We can ensure a positive coefficient scheme by using the method introduced in (Wang and Forsyth, 2008).

4.2 Matrix Form of the Discrete Equations

It will be convenient to use matrix notation for equations (4.7) and (4.8), coupled with boundary conditions.

If a Dirichlet condition is specified at $z = z_{\min}, \tau = \tau^n$ ($i = 0$), then we denote this value by G_0^n . If a Dirichlet boundary condition is specified at $z = z_{\max}, \tau = \tau^n$ ($i = q$), then we denote this value by G_q^n . The boundary conditions at $z = z_{\min}, z_{\max}$ can be enforced by specifying a boundary condition vector $G^n = [G_0^n, 0, \dots, 0, G_q^n]'$. Following the approach in (Wang and Forsyth, 2008), we can write the discrete equations (4.7) as

$$\begin{aligned} [I - \Delta\tau A^{n+1}(P^{n+1})] V^{n+1} &= V^n + (G^{n+1} - G^n), \\ \text{with } p_i^{n+1} &= \arg \min_{P \in \hat{P}} \left\{ (\mathcal{L}_h^P V^{n+1})_i \right\}, \end{aligned} \quad (4.11)$$

where

$$\begin{aligned} [A^n(P^n)V^n]_i &= (\mathcal{L}_h^{P^n} V^n)_i \\ &= [\alpha_i^n V_{i-1}^n + \beta_i^n V_{i+1}^n - (\alpha_i^n + \beta_i^n) V_i^n]; \quad 1 < i < q. \end{aligned} \quad (4.12)$$

Note that the discrete equations (4.11) are nonlinear since $P^{n+1} = P^{n+1}(V^{n+1})$. The first and last rows of A are modified as needed to handle the boundary conditions. If a Dirichlet condition

is specified at $i = 0$, we set G_0^n to the appropriate value, and set the first row in A^n to be zero. With a slight abuse of notation, we denote this last row in this case as $(A^n)_0 \equiv 0$. Conversely, if no boundary condition is required at $i = 0$, then we use forward differencing at node $i = 0$ (which means that $\alpha_0 = 0$), and set $G_0^n = 0$. The boundary condition at $z = z_{\max}$, $i = q$, is handled in a similar fashion.

The discrete equations (4.8) can be written as

$$[I - \Delta\tau A^{n+1}(P^{n+1})] U^{n+1} = U^n + (H^{n+1} - H^n), \quad (4.13)$$

where P^{n+1} is given from the discrete equations (4.11), and H encodes the boundary conditions.

4.3 Convergence to the Viscosity Solution

PDE (4.5) is linear, since the optimal control is pre-computed. We can then obtain a classical solution of the linear PDE (4.5). However, PDE (4.4) is highly nonlinear, so the classical solution may not exist in general. In this case, we are seeking the viscosity solution (Barles, 1997; Crandall et al., 1992).

In (Pooley et al., 2003), examples were given in which seemingly reasonable discretizations of nonlinear option pricing PDEs were unstable or converged to the incorrect solution. It is important to ensure that we can generate discretizations which are guaranteed to converge to the viscosity solution (Barles, 1997; Crandall et al., 1992). Assuming that equation (4.4) satisfies the strong comparison property (Barles and Burdeau, 1995; Barles, 1997; Chaumont, 2004), then, from (Barles and Souganidis, 1991; Barles, 1997), a numerical scheme converges to the unique viscosity solution if the method is pointwise consistent, stable (in the l_∞ norm) and monotone.

It is straightforward, using the methods in (Barles and Jakobsen, 2005; Forsyth and Labahn, 2008) to show that scheme (4.7) is monotone, pointwise consistent, and stable.

Assumption 4.1 (Strong Comparison) *We assume that equation (4.4) satisfies the strong comparison property.*

Remark 4.3 *If the control p is bounded, then from the results in (Chaumont, 2004; Barles and Rouy, 1998) we can deduce that Equation (4.4) satisfies the strong comparison property on the localized computational domain $\hat{\mathbb{D}}$. In the unbounded control case, we violate one of the assumptions in (Barles and Rouy, 1998) used in the proof of the strong comparison property. However, our numerical results indicate that (pw) is always bounded. Hence, in the unbounded control case, we could reformulate the problem in terms of a control (pw) , and solve the problem with assumed bounds on (pw) , which would then satisfy the conditions in (Barles and Rouy, 1998). However, it is not obvious how to obtain a priori bounds for (pw) . In practical cases, we are more interested in bounded controls, so in this case we have that strong comparison holds.*

Theorem 4.1 (Convergence to the Viscosity Solution) *Provided that the original HJB satisfies Assumption 4.1, the boundary conditions given in Section 2.2 (or 3) and discretization (4.11) satisfies the positive coefficient condition (4.10) then scheme (4.11) converges to the viscosity solution of equation (4.4).*

Proof. Using the methods in (Barles and Jakobsen, 2005; Forsyth and Labahn, 2008), this can be shown to follow from results in (Barles and Souganidis, 1991; Barles, 1997). We give a brief overview of the proof.

Monotonicity: From the positive coefficient condition (equation (4.10)) and following the same method as in (Forsyth and Labahn, 2008), we can show that scheme (4.11) is monotone.

Pointwise consistency: From Appendix A, a simple Taylor series verifies consistency. Note that since we have either simple Dirichlet conditions, or the PDE at the boundary is the limit from the interior, then we need only use the classical definition of consistency here, not the more complex version discussed in (Barles and Souganidis, 1991; Barles, 1997; Chen and Forsyth, 2008).

Stability: Using the same technique as in (Forsyth and Labahn, 2008), we can show that scheme (4.11) is l_∞ stable by a maximum analysis. Again, this is a direct consequence of the positive coefficient condition (4.10).

Under Assumption 4.1, there exists a unique, continuous viscosity solution to equation (4.4). Consequently, as shown in (Barles and Souganidis, 1991), if a discretization scheme is monotone, pointwise consistent and l_∞ stable, then that scheme converges to the unique, continuous viscosity solution. \square

4.4 Policy Iteration

Although we have established that discretization (4.11) is consistent, l_∞ stable and monotone, it is not obvious that this is a practical scheme, since the implicit timestepping method requires solution of highly nonlinear algebraic equations at each timestep.

Consider the following policy iteration scheme:

Iterative Solution of the Discrete Equations

Let $(V^{n+1})^0 = V^n$
 Let $\hat{V}^k = (V^{n+1})^k$
 For $k = 0, 1, 2, \dots$ until convergence
 Solve

$$\left[I - \Delta\tau A^{n+1}(P^k) \right] \hat{V}^{k+1} = V^n + (G^{n+1} - G^n) \tag{4.14}$$

$$p_i^k = \arg \min_{P \in \hat{P}} \left\{ (A^{n+1}(P)\hat{V}^k)_i \right\}$$
 If $(k > 0)$ and $\left(\max_i \frac{|\hat{V}_i^{k+1} - \hat{V}_i^k|}{\max(\text{scale}, |\hat{V}_i^{k+1}|)} < \text{tolerance} \right)$ then quit
 EndFor

The term *scale* in scheme (4.14) is used to ensure that unrealistic levels of accuracy are not required when the value is very small. Typically, we use $scale = 1$ in this paper, and $tolerance = 10^{-6}$.

Theorem 4.2 (Convergence of Iteration (4.14)) *If the discretization (4.11) satisfies the positive coefficient condition (4.10), then the policy iteration (4.14) converges to the unique solution of equation (4.11) for any initial iterate \hat{V}^0 . Moreover, the iterates converge monotonically.*

Proof. The proof is given in (Wang and Forsyth, 2008). □

Remark 4.4 *An important step in iteration (4.14) is to determine the optimal control p_i^k for each node i at each iteration. For the problems we study in this paper, the objective function $(\mathcal{L}_h^{P^{n+1}} V^{n+1})_i$ is a piecewise quadratic function of the control. The optimal control at each node can then be easily determined.*

In the case where the objective function is a complicated function of the control, it may be difficult to determine the optimal control analytically. If the control set \mathbb{P} is bounded, then we can replace the set of admissible controls \mathbb{P} by an approximation $\hat{\mathbb{P}}$. In this case, we define $\hat{\mathbb{P}} = [q_0, q_1, \dots, q_m]$, where $q_0 = p_{\min}$, $q_m = p_{\max}$, and

$$\max_i (q_{i+1} - q_i) = h . \tag{4.15}$$

As long as $h \rightarrow 0$ as the mesh and timesteps tend to zero, then replacing \mathbb{P} by $\hat{\mathbb{P}}$ is a consistent approximation (Wang and Forsyth, 2008), and hence converges to the viscosity solution.

Remark 4.5 *We follow the approach given in (Wang and Forsyth, 2008), which uses central differencing as much as possible, to ensure a positive coefficient scheme with a maximal use of a second order method in the W (or X) direction. When we use central differencing as much as possible, the local objective function at each node is a discontinuous function of the control. However, (Wang and Forsyth, 2008) shows that the proof of convergence of the iterative scheme for solution of the fully implicit discretized algebraic equations does not require continuity of the local objective function. Hence convergence of the iterative algorithm for solving the nonlinear discretized equations is guaranteed.*

5 Algorithm for Construction of the Efficient Frontier

Given an initial value \hat{z}_0 , Algorithm (5.1) is used to obtain the efficient frontier. Since the Z grid is discretized over the interval $[z_{\min}, z_{\max}]$, we can use Algorithm (5.1) to obtain the efficient frontier for any initial wealth $\hat{z}_0 \in [z_{\min}, z_{\max}]$ by interpolation. Of course, if we choose \hat{z}_0 to be a node in the discretized Z grid, then there is no interpolation error.

Algorithm for Constructing the Efficient Frontier

For $\gamma = \gamma_{min}, \gamma_1, \dots, \gamma_{max}$
 For timestep $n = 1, \dots, N$
 Solve equation (4.11) by using policy iteration (4.14)
 Solve equation (4.13) // P^{n+1} is given from the solution of equation (4.11)
 EndFor
 Given the initial \hat{z}_0 , use interpolation to get the value of
 $(E_{p^*}^{t=0}[Z_T], E_{p^*}^{t=0}[(Z_T - \frac{\gamma}{2})^2])_\gamma$ at $Z(t=0) = \hat{z}_0$
 If $(\frac{\gamma}{2} - E_{p^*}^{t=0}[Z_T])_\gamma > 0$ // possible valid point $\lambda > 0$
 Solve equations (2.16) to get $(E_{p^*}^{t=0}[Z_T], E_{p^*}^{t=0}[Z_T^2])_\gamma$
 Calculate the pair $(\text{Std}_{p^*}^{t=0}[Z_T], E_{p^*}^{t=0}[Z_T])_\gamma$
 EndIf
 EndFor
 Construct the upper convex hull of the points
 $(\text{Std}_{p^*}^{t=0}[Z_T], E_{p^*}^{t=0}[Z_T])_\gamma, \gamma \in [\gamma_{min}, \gamma_{max}]$ (5.1)

In Algorithm (5.1), we trace out the efficient frontier by varying $\gamma \in [\gamma_{min}, \gamma_{max}]$. Heuristic methods can be used to estimate $\gamma_{min}, \gamma_{max}$. These choices are not crucial, since we will detect invalid values of γ from the condition that $\lambda > 0$. For example, in the wealth case, to determine γ_{min} , we consider the left most point on the efficient frontier. If $\lambda \rightarrow \infty$, then the investor seeks to minimize risk. Obviously, in this case, the investor would invest all her wealth in the risk free bond at all times. In this case, her terminal wealth would be $\hat{w}_0 e^{rT} + \pi \frac{e^{rT} - 1}{r}$ with zero standard deviation. Then theoretically,

$$\gamma_{min} = 2(\hat{w}_0 e^{rT} + \pi \frac{e^{rT} - 1}{r}) . \quad (5.2)$$

There is no upper bound for γ . In particular, if there is no upper bound for the control p , there are no upper bounds for $\text{Std}_{p^*}^{t=0}[W_T]$ and $E_{p^*}^{t=0}[W_T]$ either. From our numerical tests, we find that $\gamma_{max} = 50$ is large enough to plot the efficient frontier over a reasonable range of interest.

The last step in Algorithm (5.1) is to draw the efficient frontier, given a set of candidate points. As mentioned in Remark 2.1, to find the efficient frontier for the original optimization problem (2.4), we construct an upper convex hull from the candidate points $(\text{Std}_{p^*}^{t=0}[W_T], E_{p^*}^{t=0}[W_T])$ obtained by varying γ .

6 Numerical Results

In this section, we carry out numerical tests for the defined contribution pension plan problem. We examine both the wealth case (addressed in Section 2) and the wealth-to-income ratio case (addressed in Section 3).

6.1 Wealth Case

6.1.1 Allowing Bankruptcy

r	0.03	ξ_1	0.33
σ_1	0.15	π	0.1
T	20 years	$W(t=0)$	1

TABLE 2: Parameters used in the pension plan examples.

We first examine the wealth case with bankruptcy allowed. Parameters in Table 2 are used for numerical tests. We use $w_{\max} = |w_{\min}| = 5925$ and $tolerance = 10^{-6}$ (see Algorithm (4.14)). We test a special case first, in which the variance is zero ($\lambda \rightarrow +\infty$). From equation (2.27), the analytic solution is $(\text{Std}_{p^*}^{t=0}[W_T], E_{p^*}^{t=0}[W_T]) = (0, 4.5625)$. Moreover, in this case, $\gamma = 2E_{p^*}^{t=0}[W_T]$, so $E_{p^*}^{t=0}[(X_T - \frac{\gamma}{2})^2] = 0$. We use a finite difference method with fully implicit timestepping to solve this problem numerically. We analytically determine the local optimal control at each node (as required in Algorithm 4.14).

Table 3 and 4 show the numerical results. Table 3 reports the value of $E_{p^*}^{t=0}[(X_T - \frac{\gamma}{2})^2]$, which is the viscosity solution of nonlinear HJB PDE (2.11). Table 4 reports the value of $E_{p^*}^{t=0}[W_T]$, which is the solution of the linear PDE (2.14). Given $E_{p^*}^{t=0}[(X_T - \frac{\gamma}{2})^2]$ and $E_{p^*}^{t=0}[W_T]$, the standard deviation is can be easily computed, which is also reported in Table 4. The results show that the numerical solutions of $E_{p^*}^{t=0}[(X_T - \frac{\gamma}{2})^2]$ and $E_{p^*}^{t=0}[W_T]$ converge to the analytic values at a first order rate as mesh and timestep size tends to zero. Let

$$\max_i (w_{i+1} - w_i) = O(h) \ ; \ \Delta\tau = O(h) \tag{6.1}$$

where h is the discretization parameter, then from Table 4, we see that the standard deviation converges at a rate $O(h^{1/2})$. The total number of nonlinear iterations shown in Table 3 is about two or three times of the number of timesteps. Hence, the iteration scheme (4.14) converges rapidly.

For another example, let $\lambda = 1.762$ in problem (2.4). The analytic solution given by equation (2.27) is $(\text{Std}_{p^*}^{t=0}[W_T], E_{p^*}^{t=0}[W_T]) = (0.831, 6.945)$. Tables 5 and 6 show the numerical results. The numerical solutions for $E_{p^*}^{t=0}[(X_T - \frac{\gamma}{2})^2]$ and $E_{p^*}^{t=0}[W_T]$ converge to the analytic solution at a first order rate as $h \rightarrow 0$. Figure 2 shows an efficient frontier at $(W = 1, t = 0)$, which is a straight line as expected.

Note that according to equation (2.27), if the market price of risk ξ_1 is fixed, the value of stock volatility σ_1 has no effect on the efficient frontier. When we reproduce Table 3, 4, 5 and 6 by using parameters in Table 2 but with different volatilities σ_1 , we obtain the same solutions. Hence, our numerical solutions agree on this property. However, we will see in later sections that this property may not hold when additional constraints are added to the optimal policy.

Nodes (W)	Timesteps	Nonlinear iterations	Normalized CPU Time	$E_{p^*}^{t=0}[(W_T - \frac{\gamma}{2})^2]$	Ratio
728	160	480	1	0.0818318	
1456	320	960	4.42	0.0409428	
2912	640	1295	13.21	0.0204766	1.998
5824	1280	2561	52.82	0.0102394	1.999
11648	2560	5120	213.98	0.0051200	2.000
23296	5120	10240	888.49	0.0025601	2.000

TABLE 3: *Convergence study. Use analytic solution for the optimal control at each node. Fully implicit timestepping is applied, using constant timesteps. Parameters are given in Table 2, with $\gamma = 9.125$. Values of $E_{p^*}^{t=0}[(W_T - \frac{\gamma}{2})^2]$ are reported at $(W = 1, t = 0)$. Ratio is the ratio of successive changes in the computed values for decreasing values of the discretization parameter h . Analytic solution is $E_{p^*}^{t=0}[(W_T - \frac{\gamma}{2})^2] = 0$. CPU time is normalized. We take the CPU time used for the first test in this table as one unit of CPU time, which uses 728 nodes for the W grid and 160 timesteps.*

Nodes (W)	Timesteps	$\text{Std}_{p^*}^{t=0}[W_T]$	$E_{p^*}^{t=0}[W_T]$	Ratio for $\text{Std}_{p^*}^{t=0}[W_T]$	Ratio for $E[W_T]$
728	160	0.285617	4.54653		
1456	320	0.202202	4.55494		
2912	640	0.143039	4.55845	1.410	2.396
5824	1280	0.101166	4.56031	1.413	1.887
11648	2560	0.071547	4.56148	1.414	1.590
23296	5120	0.050595	4.56200	1.414	2.250

TABLE 4: *Convergence study. Use analytic solution for the optimal control at each node. Fully implicit timestepping is applied, using constant timesteps. Parameters are given in Table 2, with $\gamma = 9.125$. Values of $\text{Std}_{p^*}^{t=0}[W_T]$ and $E_{p^*}^{t=0}[W_T]$ are reported at $(W = 1, t = 0)$. Ratio is the ratio of successive changes in the computed values for decreasing values of the discretization parameter h . Analytic solution is $(\text{Std}_{p^*}^{t=0}[W_T], E_{p^*}^{t=0}[W_T]) = (0.0, 4.5625)$.*

As mentioned in Section 2.2.1, some error is introduced using the artificial boundaries w_{\min} and w_{\max} , which approximate infinite boundaries. However, we can make these errors small by choosing large values for $(|w_{\min}|, w_{\max})$. Table 7 shows the values of $E_{p^*}^{t=0}[(W_T - \frac{\gamma}{2})^2]$ and $E_{p^*}^{t=0}[W_T]$ for different large boundaries. We can see that once $(|w_{\min}|, w_{\max})$ are large enough, the values of $E_{p^*}^{t=0}[(W_T - \frac{\gamma}{2})^2]$ and $E_{p^*}^{t=0}[W_T]$ are insensitive to the location of these large boundaries.

6.1.2 Bounded Control

In this section, we examine the wealth case with bounded control $\mathbb{P} = [0, 1.5]$. There is no analytic solution in this case. The efficient frontier is shown in Figure 3, with $(W(t=0) = 1, t = 0)$. We also show the efficient frontiers for $\mathbb{D} \in [0, +\infty)$ and $\mathbb{P} = [0, +\infty)$, the *no bankruptcy* case, and for the case where bankruptcy is allowed, $\mathbb{D} = (-\infty, +\infty)$ and $\mathbb{P} = (-\infty, +\infty)$. Clearly, the strategy given by the allowing bankruptcy case is the most efficient, and the strategy given by the bounded

Nodes (W)	Timesteps	Nonlinear iterations	Normalized CPU Time	$E_{p^*}^{t=0}[(W_T - \frac{\gamma}{2})^2]$	Ratio
728	160	480	1.11	0.934593	
1456	320	855	4.05	0.852331	
2912	640	1280	12.95	0.812095	2.045
5824	1280	2560	54.16	0.792530	2.057
11648	2560	5120	222.56	0.783030	2.059

TABLE 5: *Convergence study. Use analytic solution for the optimal control at each node. Fully implicit timestepping is applied, using constant timesteps. Parameters are given in Table 2, with $\lambda = 1.762$ ($\gamma = 14.47$). Values of $E_{p^*}^{t=0}[(X_T - \frac{\gamma}{2})^2]$ are reported at $(W = 1, t = 0)$. Ratio is the ratio of successive changes in the computed values for decreasing values of the discretization parameter h . CPU time is normalized. We take the CPU time used for the first test in Table 3 as one unit of CPU time, which uses 728 nodes for the W grid and 160 timesteps.*

Nodes (W)	Timesteps	$\text{Std}_{p^*}^{t=0}[W_T]$	$E_{p^*}^{t=0}[W_T]$	Ratio for $\text{Std}_{p^*}^{t=0}[W_T]$	Ratio for $E[W_T]$
728	160	0.915441	6.92426		
1456	320	0.872917	6.93442		
2912	640	0.851483	6.93992	1.975	1.847
5824	1280	0.840821	6.94251	2.007	2.124
11648	2560	0.835612	6.94383	2.045	1.962

TABLE 6: *Convergence study. Use analytic solution of the optimal control at each node. Fully implicit timestepping is applied, using constant timesteps. Parameters are given in Table 2, with $\lambda = 1.762$ ($\gamma = 14.47$). Values of $\text{Std}_{p^*}^{t=0}[W_T]$ and $E_{p^*}^{t=0}[W_T]$ are reported at $(W = 1, t = 0)$. Ratio is the ratio of successive changes in the computed values for decreasing values of the discretization parameter h . Analytic solution: $(\text{Std}_{p^*}^{t=0}[W_T], E_{p^*}^{t=0}[W_T]) = (0.831, 6.945)$.*

Nodes (W)	(w_{\min}, w_{\max})	$E_{p^*}^{t=0}[(W_T - \frac{\gamma}{2})^2]$	$E_{p^*}^{t=0}[W_T]$
11648	(-5925, 5925)	0.783030	6.94383
11904	(-11953, 11953)	0.783030	6.94383
12160	(-23906, 23906)	0.783030	6.94383
12672	(-47869, 47869)	0.783030	6.94383

TABLE 7: *Effect of finite boundary. Parameters are given in Table 2, with $\gamma = 14.47$. There are 2560 timesteps for each test.*

control case is the least efficient.

As discussed in Section 6.1.1, in the case of allowing bankruptcy, if the market price of risk ξ_1 is fixed, the value of stock volatility σ_1 has no effect on the efficient frontier. However, this property may not hold when additional constraints are added on the optimal policy. For example, in the case of bounded control, the efficient frontier will move upward, if the value of σ_1 increases with ξ_1 fixed (this makes the stock drift rate $\mu_S = r + \xi_1\sigma_1$ increase). This result is illustrated in Figure 4 (a). However, if the value of σ_1 increases with μ_S fixed (this makes ξ_1 decrease), the efficient

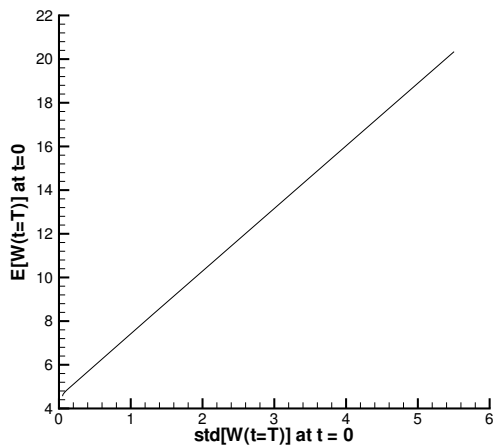


FIGURE 2: *Efficient frontier. Parameters are given in Table 2. Values are reported at $(W = 1, t = 0)$.*

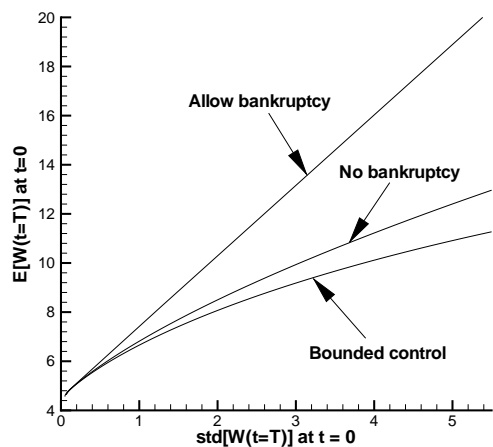


FIGURE 3: *Efficient frontiers (wealth case) for allowing bankruptcy ($\mathbb{D} = (-\infty, +\infty)$ and $\mathbb{P} = (-\infty, +\infty)$), no bankruptcy ($\mathbb{D} = [0, +\infty)$ and $\mathbb{P} = [0, +\infty)$) and bounded control ($\mathbb{D} = [0, +\infty)$ and $\mathbb{P} = [0., 1.5]$) cases. Parameters are given in Table 2. Values are reported at $(W = 1, t = 0)$.*

frontier will move downward. This result is illustrated in Figure 4 (b).

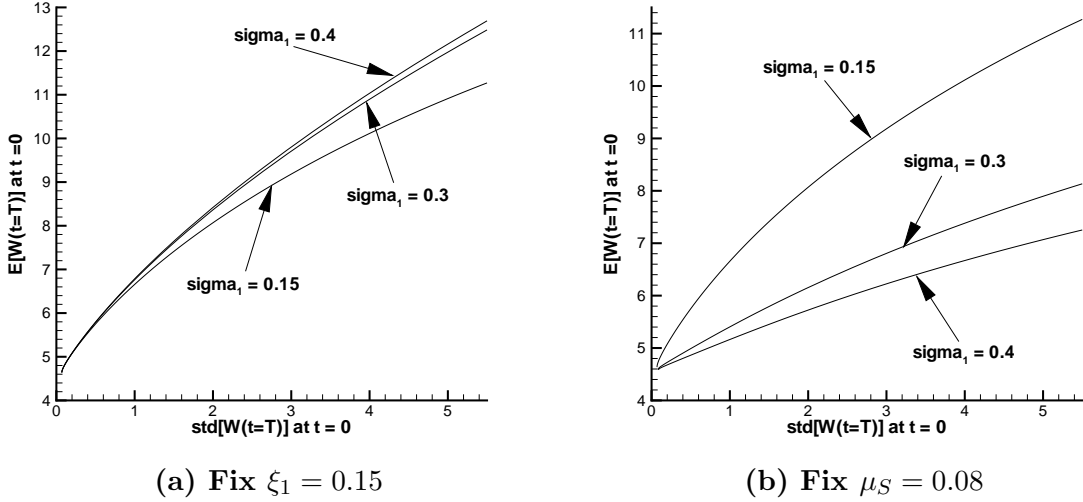


FIGURE 4: Efficient frontiers for various values of stock volatilities. Parameters are given in Table 2, in particular $W(t=0) = 1$, $\mathbb{D} = [0, +\infty)$ and $\mathbb{P} = [0, 1.5]$. Figure (a) shows the efficient frontiers for different volatilities with a fixed market price of risk $\xi_1 = 0.15$. Figure (b) shows the efficient frontiers for different volatilities with a fixed stock drift rate $\mu_S = 0.08$.

6.1.3 Multi-period Portfolio Selection Problem

In Section 2.4, we show that the pension plan problem can be reduced to the classic multi-period portfolio selection problem by simply setting the contribution rate $\pi = 0$. Of course, when $\pi = 0$, the efficient frontier is still a straight line in this case from equation (2.27) for the case of allowing bankruptcy. In this section, we examine the case of no bankruptcy, where $\mathbb{D} = [0, +\infty)$ and $\mathbb{P} = [0, +\infty)$. An analytic solution is given for the no bankruptcy case in (Bielecki et al., 2005). We can show numerically that the efficient frontier given by our approach converges to the analytic solutions given in (Bielecki et al., 2005). Using the parameters in (Bielecki et al., 2005; Zhou and Li, 2000) ($r = 0.06$, $\sigma_1 = 0.15$, $\xi_1 = 0.4$, $T = 1$ and $W(t=0) = 1$), Figure 5 shows the efficient frontiers. The straight line is for the case of unbounded control, allowing bankruptcy, which is obtained from equation (2.27). The curves below the straight line are actually two overlapping curves. One of them is obtained from the analytic solution given in (Bielecki et al., 2005), and the other is obtained from the numerical solutions by our approach. Figure 5 clearly shows that our numerical solutions converge to the analytic curve. Note that as discussed in Section 2.4, the approach given in (Bielecki et al., 2005) uses the monetary amount as the control, but our method uses the proportion as the control. Figure 5 shows that the two methods produce the same solutions in terms of efficient frontier. We remind the reader that since we allow p be unbounded, it is possible that the wealth can be zero before the terminal time. However, our numerical results appear to indicate that the optimal policy is such that this will not occur, (see Remark 6.1) thus verifying a conjecture in (Bielecki et al., 2005).

In (Li and Zhou, 2006), the authors discuss an 80% rule for continuous time mean variance

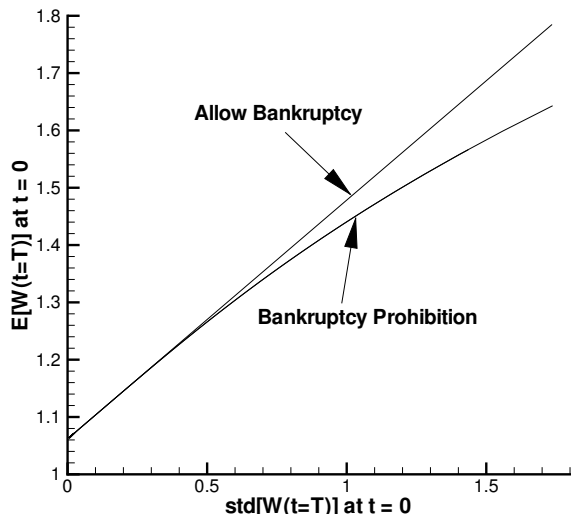


FIGURE 5: *Efficient frontiers for multi-period portfolio selection problems. The straight line is for the case of allowing bankruptcy, which is obtained from equation (2.27). The curve below the straight line is actually two overlapping curves. One of them is obtained from the analytic solution given in (Bielecki et al., 2005), and the other is obtained from the numerical solutions by our approach. Parameters are $r = 0.06$, $\sigma_1 = 0.15$, $\xi_1 = 0.4$, $T = 1$ and $W(t = 0) = 1$. Values are reported at $(W = 1, t = 0)$.*

efficiency. This rule states that in the case of allowing bankruptcy ($\mathbb{D} = (-\infty, +\infty)$ and $\mathbb{P} = (-\infty, +\infty)$), given any target terminal wealth, say \hat{g} ($> W(t = 0)e^{rT}$), where $\hat{g} = E_{p^*}^{t=0}[W_T]$, there is at least an 80% probability that the optimal strategy will reach the target over the time horizon $[0, T]$. This result may be surprising at first glance. The cost of this surprising rule is the high probability of bankruptcy when the target terminal wealth is high. We use Monte-Carlo simulations to examine this rule. Using the same parameters as used to construct Figure 5, we solve the stochastic optimal control problem (2.4) with Algorithm (5.1) (we choose a γ such that $E_{p^*}^{t=0}(W_T) = \hat{g}$), and store the optimal strategies for each $(W = w, t)$. We then carry out Monte-Carlo simulations based on the stored strategies with $W(t = 0) = 1$ initially. As mentioned in (Li and Zhou, 2006), at any time $t \in [0, T]$, once the investor's wealth $W(t) \geq \hat{g}e^{-r(T-t)}$, the investor will switch all her wealth into bonds, so that her final wealth $W_T \geq \hat{g}$. Note that this simulation strategy is slightly different from the pre-commitment strategy. With a pre-commitment strategy, the investor commits to the pre-computed strategy until $t = T$ irregardless of reaching the investment target. Table 8 shows the result of Monte-Carlo simulations. We see that no matter how large the target wealth, the probability of success (hitting the target wealth) is higher than 80%. However, when the target wealth is high, the probability of bankruptcy is also very high. Note that at any time $t \in [0, T]$, if $W(t) \leq 0$, bankruptcy occurs. But since bankruptcy is allowed, the investor can still borrow money and continue investing. This may result in positive wealth at

some later time. The last column in Table 8 shows the probability of bankruptcy at time T , which is much lower than the probability of bankruptcy at any time $t \in [0, T]$.

Table 8 also examines the probability of hitting the target for the bankruptcy prohibition case and the bounded control case. The results show that the 80% rule does not hold for these two cases. When the target wealth increases, the probability of hitting the target decreases, but the probability of bankruptcy is zero.

$E_{p^*}^{t=0}[W_T] = \hat{g}$	$\text{Std}_{p^*}^{t=0}[W_T]$	Success investment	Bankruptcy at any time t	Bankruptcy at time T
Bankruptcy is allowed: $\mathbb{D} = (-\infty, +\infty)$ and $\mathbb{P} = (-\infty, +\infty)$				
1.19979	0.33123	82.3984%	1.3063%	0.5297%
2.00060	2.25380	82.2125%	38.7344%	10.6656%
4.60097	8.49677	82.3922%	69.7328%	14.1094%
Bankruptcy prohibition: $\mathbb{D} = [0, +\infty)$ and $\mathbb{P} = [0, +\infty)$				
1.19994	0.33348	82.7866%	0	0
2.00199	3.69090	63.8516%	0	0
3.06641	20.66430	43.9625%	0	0
Bounded control: $\mathbb{D} = [0, +\infty)$ and $\mathbb{P} = [0, 1.5]$				
1.08225	0.04908	82.5922%	0	0
1.16185	0.26486	74.9141%	0	0

TABLE 8: 80% rule study. Parameters used as in (Bielecki et al., 2005; Zhou and Li, 2000) ($r = 0.06$, $\sigma_1 = 0.15$, $\xi_1 = 0.4$, $T = 1$ and $W(t = 0) = 1$). 64,000 Monte-Carlo simulations for each test. 512 Monte-Carlo timesteps are used for allowing bankruptcy case and bounded control case, and 25600 timesteps are used for no bankruptcy case. Success is defined as $W(t) \geq E_{p^*}^{t=0}(W_T)e^{-r(T-t)}$, $t \leq T$.

Remark 6.1 In the case of bankruptcy prohibition, $\lim_{w \rightarrow 0}(p^*w) = 0$. Our numerical tests show that as w goes to zero, $p^*w = O(w^\beta)$. For the a reasonable range of parameters, $\beta \simeq 0.95 \pm 0.02$. As discussed in (Kahl et al., 2008), zero is an unattainable boundary for the stochastic process (2.29) if $\beta > .5$. We apply an explicit Milstein method (Kahl et al., 2008) when carrying out Monte-Carlo simulations to ensure that zero is unattainable. The explicit Milstein method requires some timestep size restrictions. As a result, we use a small timestep size ($\frac{1}{25600}$ year) for the no bankruptcy case in simulations. Although zero is unattainable for the bounded control case, we do not have to use the Milstein method. Since the control p is capped at 1.5, as $w \rightarrow 0$, p^*w goes to zero as the same rate as w . We do not observe any difficulties in this case using the standard explicit Euler scheme.

6.2 Wealth-to-income Ratio Case

In this Section, we examine the wealth-to-income ratio case. We use parameters in Table 9, and our finite difference method for solution of the optimal stochastic control problem (3.5). We set $x_{\max}, |x_{\min}| = 1000$ in this case, and $\text{tolerance} = 10^{-6}$ in Algorithm (4.14). Increasing x_{\max} had no effect on the solution to six digits. There is no known analytic solution for this case. A convergence study is shown in Tables 10 and 11. Table 10 reports the values of $E_{p^*}^{t=0}[(X_T - \frac{\gamma}{2})^2]$, and Table 11

μ_y	0.	ξ_1	0.2
σ_1	0.2	σ_{Y1}	0.05
σ_{Y0}	0.05	π	0.1
T	20 years	γ	15
\mathbb{P}	$[0, 1.5]$	\mathbb{D}	$[0, +\infty)$

TABLE 9: Parameters used in the pension plan examples.

reports the values of $\text{Std}_{p^*}^{t=0}[X_T]$ and $E_{p^*}^{t=0}[X_T]$. Both tables show a first order convergence rate as $h \rightarrow 0$.

Nodes (X)	Timesteps	Nonlinear iterations	Normalized CPU Time	$E_{p^*}^{t=0}[(X_T - \frac{\gamma}{2})^2]$	Ratio
89	40	100	1	15.9197	
177	80	166	4.08	15.7498	
353	160	320	13.27	15.6682	2.082
705	320	640	53.06	15.6272	1.990
1409	640	1280	205.10	15.6066	1.990
2817	1280	2560	841.84	15.5963	2.000

TABLE 10: Convergence study. The optimal control at each node is computed using analytic methods. Fully implicit timestepping is applied, using constant timesteps. Parameters are given in Table 9. Values of $E_{p^*}^{t=0}[(X_T - \frac{\gamma}{2})^2]$ are reported at $(X = 0.5, t = 0)$. Ratio is the ratio of successive changes in computed values as $h \rightarrow 0$. CPU time is normalized. We take the CPU time used for the first test in this table as one unit of CPU time, which uses 89 nodes for the X grid and 40 timesteps.

Nodes (X)	Timesteps	$\text{Std}_{p^*}^{t=0}[X_T]$	$E_{p^*}^{t=0}[X_T]$	Ratio for $\text{Std}_{p^*}^{t=0}[X_T]$	Ratio for $E_{p^*}^{t=0}[X_T]$
89	40	1.80509	3.94173		
177	80	1.77167	3.94881		
353	160	1.75521	3.95213	2.030	2.133
705	320	1.74692	3.95381	1.986	1.976
1409	640	1.74276	3.95467	1.993	1.953
2817	1280	1.74068	3.95509	2.000	2.048

TABLE 11: Convergence study. The optimal control at each node is computed using analytic methods. Fully implicit timestepping is applied, using constant timesteps. Parameters are given in Table 9. Values of $E_{p^*}^{t=0}[X_T]$ and $\text{Std}_{p^*}^{t=0}[X_T]$ are reported at $(X = 0.5, t = 0)$. Ratio is the ratio of successive changes in computed values as $h \rightarrow 0$.

In order to solve the HJB PDE (3.9), the optimal control p^* needs to be determined to minimize the objective function at each node. This objective function is a piecewise quadratic function of p . Hence, it is not difficult to determine the analytic solution for the control p . Values in Table 10 and 11 are obtained by using the analytic method for optimal p^* at each node. However, in some

cases, it is not easy to determine the analytic solution for the control. In such cases, the control set \mathbb{P} can be discretized to a set $\hat{\mathbb{P}}$ (as discussed in Remark 4.4), and the optimal control can be determined by linear search. The convergence to viscosity solution of this method is proven in (Wang and Forsyth, 2008). Table 12 and 13 show a convergence study with the discretized control. Again, a first order convergence rate is obtained in both tables. Of course, this method requires much more CPU time compared to the method used by Table 10 and 11. This is simply due to the comparatively crude method used to find the optimal control at each grid node.

Nodes ($X \times \hat{\mathbb{P}}$)	Timesteps	Nonlinear iterations	Normalized CPU Time	$E_{p^*}^{t=0}[(X_T - \frac{\gamma}{2})^2]$	Ratio
89×21	40	101	4.08	15.9242	
177×41	80	166	22.45	15.7509	
353×81	160	320	161.22	15.6684	2.101
705×161	320	640	1276.53	15.6272	2.002
1409×321	640	1280	9917.35	15.6066	2.000
2817×641	1280	2560	76102.04	15.5963	2.000

TABLE 12: *Convergence study. Use discretized control set $\hat{\mathbb{P}}$ and linear search to find the optimal control. Fully implicit timestepping is applied, using constant timesteps. Parameters are given in Table 9. Values of $E_{p^*}^{t=0}[(X_T - \frac{\gamma}{2})^2]$ are reported at $(X = 0.5, t = 0)$. Ratio is the ratio of successive changes in computed values as $h \rightarrow 0$. CPU time is normalized. We take the CPU time used for the first test in Table 10 as one unit of CPU time, which uses 89 nodes for X grid and 40 timesteps.*

Nodes ($X \times \hat{\mathbb{P}}$)	Timesteps	$\text{Std}_{p^*}^{t=0}[X_T]$	$E_{p^*}^{t=0}[X_T]$	Ratio for $\text{Std}_{p^*}^{t=0}[X_T]$	Ratio for $E_{p^*}^{t=0}[X_T]$
89×21	40	1.80701	3.94206		
177×41	80	1.77144	3.94854		
353×81	160	1.75529	3.95213	2.202	1.805
705×161	320	1.74693	3.95381	1.932	2.137
1409×321	640	1.74276	3.95466	2.005	1.976
2817×641	1280	1.74068	3.95509	2.005	1.977

TABLE 13: *Convergence study. Use discretized control set $\hat{\mathbb{P}}$ and linear search to find the optimal control. Fully implicit timestepping is applied, using constant timesteps. Parameters are given in Table 9. Values of $E_{p^*}^{t=0}[X_T]$ and $\text{Std}_{p^*}^{t=0}[X_T]$ are reported at $(X = 0.5, t = 0)$. Ratio is the ratio of successive changes in computed values as $h \rightarrow 0$.*

Figure 6 shows the efficient frontiers allowing bankruptcy, no bankruptcy and bounded control cases. Again, the strategy given by the allowing bankruptcy case is the most efficient, and the strategy given by the bounded control case is the least efficient.

In Section 6.1, we have discussed the effects of changing the value of σ_1 on the efficient frontier solution. We obtain similar results for the wealth-to-income case. For a fixed ξ_1 , different values of σ_1 give the same efficient frontier solution in the case of allowing bankruptcy. However, this property does not hold for the bounded control case. Figure 7 (a) illustrates that for a fixed ξ_1 ,

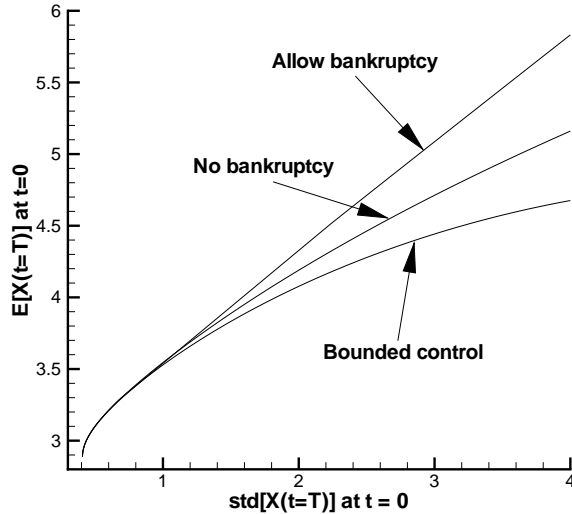


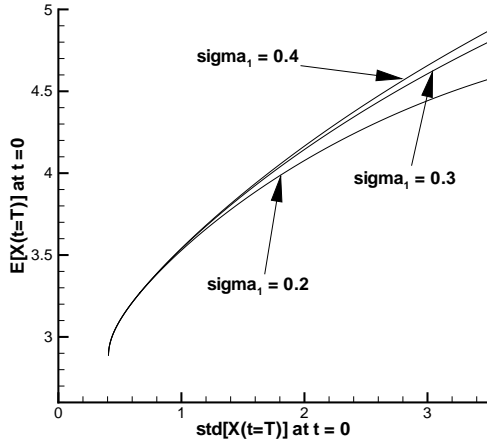
FIGURE 6: *Efficient frontiers (wealth-to-income ratio case) for allowing bankruptcy ($\mathbb{D} = (-\infty, +\infty)$ and $\mathbb{P} = (-\infty, +\infty)$), no bankruptcy ($\mathbb{D} = [0, +\infty)$ and $\mathbb{P} = [0, +\infty)$) and bounded control ($\mathbb{D} = [0, +\infty)$ and $\mathbb{P} = [0., 1.5]$) cases. Parameters are given in Table 9. Values are reported at $(X = 0.5, t = 0)$.*

increasing σ_1 moves the efficient frontier upward in the case of bounded control. Figure 7 (b) illustrates that for a fixed μ_S , increasing σ_1 moves the efficient frontier downward.

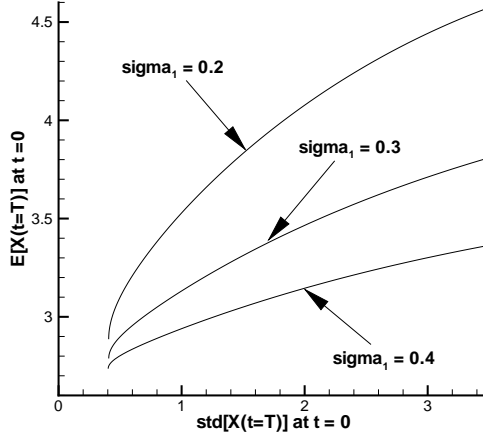
Figure 8 shows the values of the optimal control (the investment strategies) at different time t for a fixed $T = 20$ and $\gamma = 15$. Under these inputs, if $X(t = 0) = 0.5$, $(\text{Std}_{p^*}^{t=0}[X_T], E_{p^*}^{t=0}[X_T]) = (1.7407, 3.9551)$ from the finite difference solution. From this figure, we can see that the control p is an increasing function of time t for a fixed X . This is a bit counterintuitive, since one may imagine that the investor should become more conservative (switch to bonds) as time goes on. However, if total wealth-to-income ratio remains fixed as time increases, then the investor must take on more risk to have a higher probability of hitting the investment target. This behaviour of the optimal strategy is also seen in the analytic solution for the wealth case with bankruptcy allowed (Equation (2.28)).

Using the parameters in Table 9, we solve the stochastic optimal control problem (equation (3.5)) and store the optimal strategies for each $(X = x, t)$. We then carry out Monte-Carlo simulations based on the stored strategies for $X(t = 0) = 0.5$ initially. The value for $(\text{Std}_{p^*}^{t=0}[X_T], E_{p^*}^{t=0}[X_T])$ is $(1.7407, 3.9551)$ (from the finite difference solution). Table 14 shows a convergence study of Monte-Carlo simulations, and Figure 9 shows a plot of the convergence study. As the number of simulations increases and the timestep size decreases, the results given by Monte-Carlo simulation converge to the values given by solving the finite difference solution.

Figure 10 shows the probability density function of Monte-Carlo simulations (500000 simulations). Figure 10 (a) uses $\gamma = 15$ ($(\text{Std}_{p^*}^{t=0}[X_T], E_{p^*}^{t=0}[X_T]) = (1.7407, 3.9551)$), while Figure 10



(a) Fix $\xi_1 = 0.2$



(b) Fix $\mu_S = 0.04$

FIGURE 7: Efficient frontiers for various values of stock volatilities. Parameters are given in Table 9, in particular $X(t = 0) = 0.5$, $\mathbb{D} = [0, +\infty)$ and $\mathbb{P} = [0, 1.5]$. Figure (a) shows the efficient frontiers for different volatilities with a fixed market price of risk $\xi_1 = 0.2$. Figure (b) shows the efficient frontiers for different volatilities with a fixed stock drift rate $\mu_S = 0.04$.

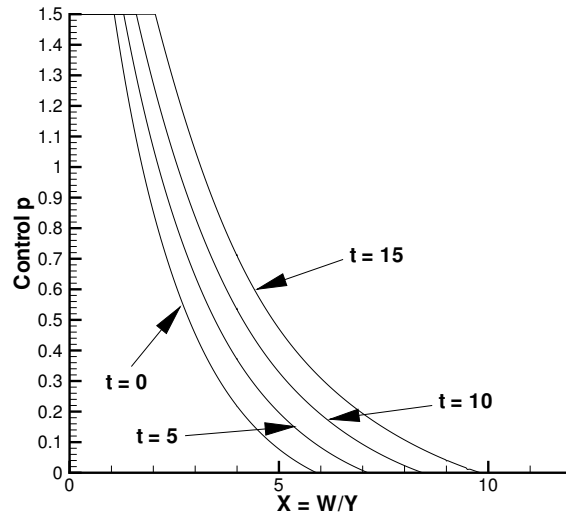


FIGURE 8: Optimal control as a function of (X, t) . Parameters are given in Table 9. Under these inputs, if $X(t = 0) = 0.5$, $(Std_{p^*}^{t=0}[X_T], E_{p^*}^{t=0}[X_T]) = (1.7407, 3.9551)$ from finite difference solution.

# of Simulations	MC Timestep	$E_{p^*}^{t=0}[X_T]$	$Std_{p^*}^{t=0}[X_T]$
1000	0.25	3.9840	1.7233
4000	0.125	3.9396	1.7305
16000	0.0625	3.9656	1.7366
64000	0.03125	3.9566	1.7381
256000	0.015625	3.9559	1.7390

TABLE 14: Convergence study for the Monte-Carlo Simulations. Parameters are given in Table 9. Values for $E_{p^*}^{t=0}[X_T]$ and $Std_{p^*}^{t=0}[X_T]$ are reported at $(X = 0.5, t = 0)$. The finite difference values are: $E_{p^*}^{t=0}[X_T] = 3.9551$ and $Std_{p^*}^{t=0}[X_T] = 1.7407$.

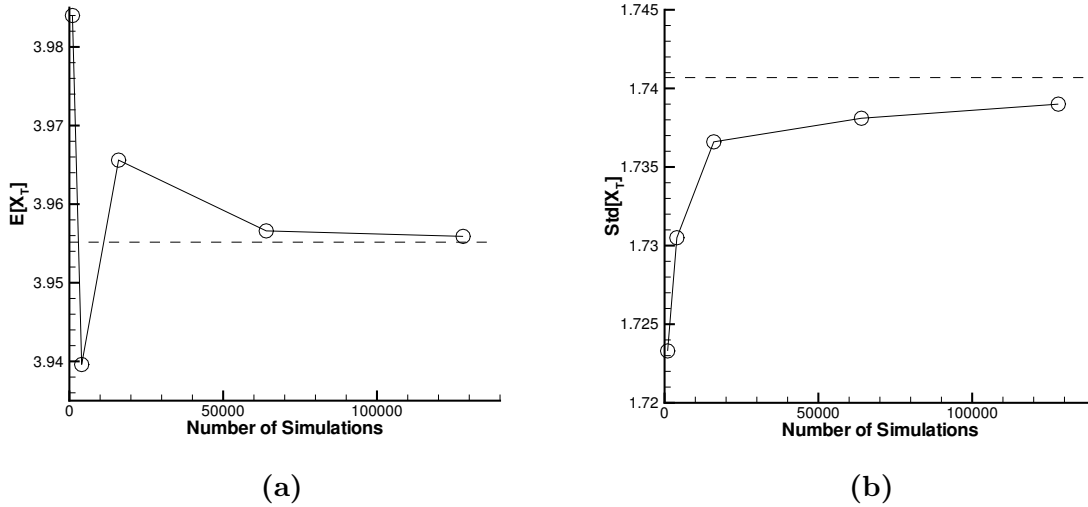


FIGURE 9: Convergence study for Monte-Carlo Simulation. Parameters are given in Table 9. Figure (a) shows the plot of $E_{p^*}^{t=0}[X_T]$. Figure (b) shows the plot for $Std_{p^*}^{t=0}[X_T]$. $E_{p^*}^{t=0}[X_T]$ and $Std_{p^*}^{t=0}[X_T]$ are written as $E[X_T]$ and $Std[X_T]$ in the figure. Values for $E_{p^*}^{t=0}[X_T]$ and $Std_{p^*}^{t=0}[X_T]$ are reported in Table 14. The finite difference values are $(Std_{p^*}^{t=0}[X_T], E_{p^*}^{t=0}[X_T]) = (1.7407, 3.9551)$.

(b) uses $\gamma = 8$ ($(Std_{p^*}^{t=0}[X_T], E_{p^*}^{t=0}[X_T]) = (0.6627, 3.2647)$). The shape of the probability density function depends on input parameters (γ in this example). Note the double peak in Figure 10(a). For this case, when the control is unconstrained ($\mathbb{P} = (-\infty, +\infty)$), the probability density function (which is not shown in this paper) has a single peak near $E_{p^*}^{t=0}[X_T]$.

However, when $\gamma = 15$, $p_{\max} = 1.5$, then the control hits the constraint (see Figure 8) for small X . Hence the investor has to choose a strategy with less than optimal (compared to the unbounded control case) expected return. As a result, there is another peak to the left of the value of $E_{p^*}^{t=0}[X_T]$ in the probability density function. If γ is small enough, the optimal strategy does not hit the constraints, and the probability density function reverts to a single peak. As shown in 10 (b), there is only one peak in the probability density function for $\gamma = 8$.

Figure 11 shows the mean and standard deviation for the strategy $p(t, x)$ as time changes.

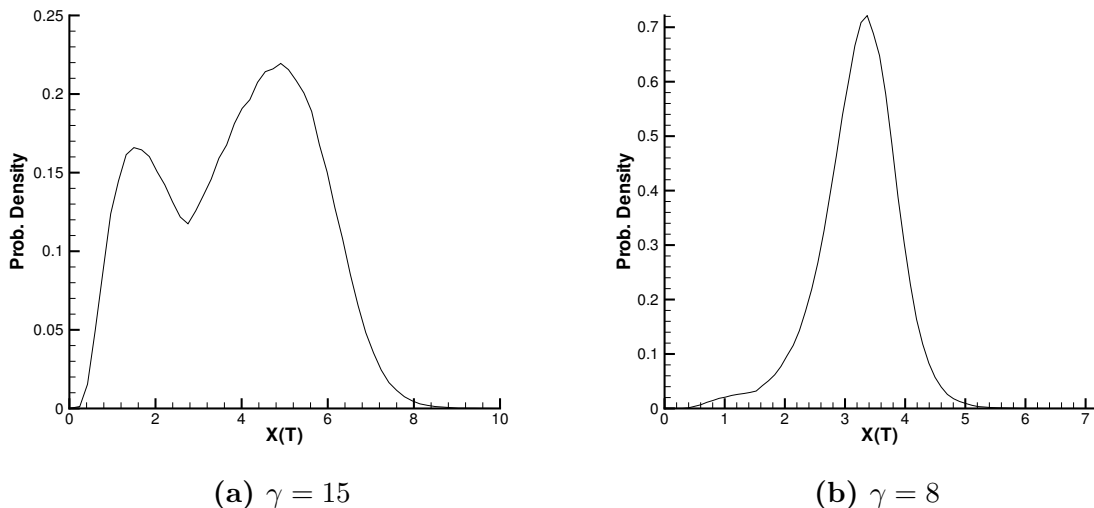


FIGURE 10: *Probability density function for Monte-Carlo Simulation, 500,000 simulations and 1280 simulation timesteps. Parameters are given in Table 9. Values for $(E_{p^*}^{t=0}[X_T], Std_{p^*}^{t=0}[X_T])$ are reported at $(X = 0.5, t = 0)$. Figure (a) uses $\gamma = 15$, while Figure (b) uses $\gamma = 8$. For Figure (a), $(Std_{p^*}^{t=0}[X_T], E_{p^*}^{t=0}[X_T]) = (1.7407, 3.9551)$ from finite difference solution; For Figure (b), $(Std_{p^*}^{t=0}[X_T], E_{p^*}^{t=0}[X_T]) = (0.6627, 3.2647)$ from finite difference solution.*

Figure 11 (a) uses $\gamma = 15$ ($(Std_{p^*}^{t=0}[X_T], E_{p^*}^{t=0}[X_T]) = (1.7407, 3.9551)$), while Figure 11 (b) uses $\gamma = 8$ ($(Std_{p^*}^{t=0}[X_T], E_{p^*}^{t=0}[X_T]) = (0.6627, 3.2647)$). Both of these Figures show that the mean of $p(t, x)$ is a decreasing function of time t , i.e., as time goes on, the investor switches into the less risky strategy (on average). Since the value of $E_{p^*}^{t=0}[X_T]$ in Figure 11 (a) is higher than the one in Figure 11 (b), the mean strategy in Figure 11 (a) is more risky compared to Figure 11 (b).

7 Conclusion

In this paper, we use a mean variance approach to find an optimal dynamic asset allocation strategy for a defined contribution pension plan. One advantage of this approach is that the results can be easily interpreted in terms of an efficient frontier, so that an investor can intuitively choose her expected return and risk level. It is well-known that dynamic programming cannot be used in straightforward fashion for constructing the efficient frontier. To avoid this difficulty, we follow the method introduced in (Zhou and Li, 2000; Li and Ng, 2000) which embeds the original optimization problem into a class of auxiliary stochastic LQ problems. Instead of solving the original problem, we can then use dynamic programming to solve the LQ problem.

We discuss two cases for the pension plan problem. In the first case, the contribution rate is a constant, and given a risk level, we construct the efficient frontier in terms of the terminal wealth. In the second case, we assume the investor contributes a constant proportion of her year salary into her pension account every year. In this case, we construct the efficient frontier in terms of the

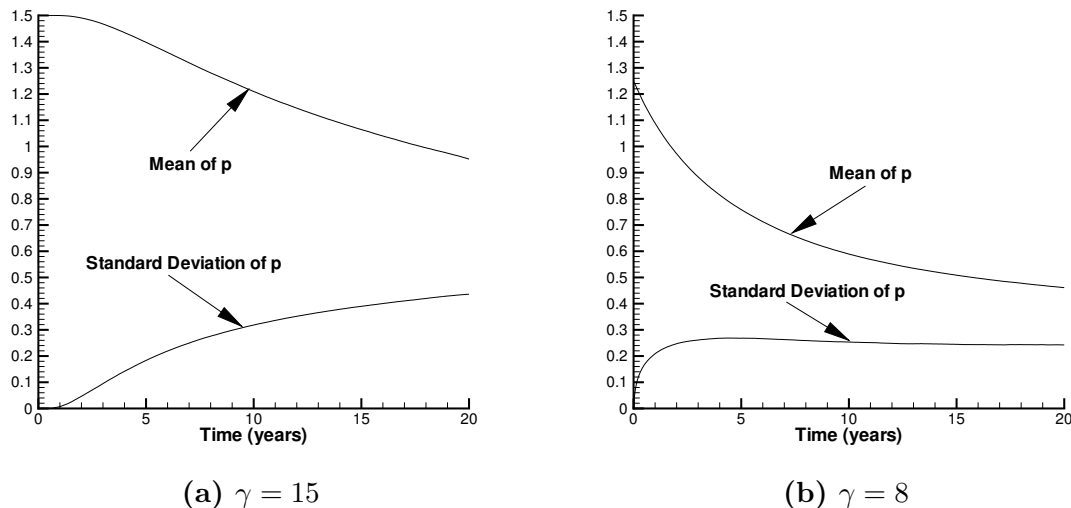


FIGURE 11: Mean and standard deviation for the control $p(t, x)$. There are 64000 simulations and 1280 simulation timesteps. Parameters are given in Table 9. Figure (a) uses $\gamma = 15$, while Figure (b) uses $\gamma = 8$. For Figure (a), $(Std_{p^*}^{t=0}[X_T], E_{p^*}^{t=0}[X_T]) = (1.7407, 3.9551)$ from finite difference solution; For Figure (b), $(Std_{p^*}^{t=0}[X_T], E_{p^*}^{t=0}[X_T]) = (0.6627, 3.2647)$ from finite difference solution.

terminal wealth-to-income ratio.

Our method can handle various constraints on the optimal policy. For the terminal wealth case, analytic solutions exist (Hojgaard and Vigna, 2007; Zhou and Li, 2000; Li and Ng, 2000) when there is no constraint on the wealth or the control, i.e., $W(t) \in (-\infty, +\infty)$ (bankruptcy is allowed) and the control $p \in (-\infty, +\infty)$ (infinite borrowing is allowed). Some analytic solutions have been developed for handling some specific constraints: no stock shorting (Li et al., 2002) and the no bankruptcy case (Bielecki et al., 2005). However, these special constraints still allow infinite borrowing, which is unlikely in practice. If the investor is restricted to borrow at most a certain proportion (e.g. 50%) of her total wealth, analytic solutions do not exist. The problem has to be solved numerically.

We develop a fully implicit method for solving the nonlinear HJB PDE, which arises in the LQ formulation of the mean variance problem. Our method satisfies sufficient conditions to ensure convergence to the viscosity solution of the HJB equation, provided the unique, continuous viscosity solution exists. The properties of the discretization also ensure that the policy iteration scheme used to solve the nonlinear algebraic equations at each timestep is globally convergent. By solving the HJB PDE and a related linear PDE, we develop an algorithm for constructing the mean variance efficient frontier. Note that a fully implicit method has no timestep size restrictions due to stability. If an explicit method were used, we would need to estimate the maximum stable timestep, which would be problematic in the case of an unbounded control.

In order to compare the numerical solution with the known analytic solution in special cases, it is necessary to allow for negative wealth and unbounded controls. This requires careful attention

to the grid construction and form of the control as the mesh and timesteps shrink to zero.

Numerical tests show that our numerical solutions converge to the analytic solution (where available). The policy iteration scheme converges very rapidly. We also examine some cases of realistic constraints where analytic solutions do not exist. From a practical point of view, we observe that the addition of realistic constraints can completely alter some of the properties of the mean variance solution compared to the unconstrained control case. For example, the efficient frontier is no longer a straight line, the frontier is sensitive to the risky asset volatility, and the 80% rule (Li and Zhou, 2006) no longer holds.

We plan to carry out a similar study of time-consistent mean variance optimal asset allocation in the near future.

A Discrete Equation Coefficients

Let p_i^n denote the optimal control p^* at node i , time level n and set

$$a_i^{n+1} = a(z_i, p_i^n), \quad b_i^{n+1} = b(z_i, p_i^n), \quad c_i^{n+1} = c(z_i, p_i^n). \quad (\text{A.1})$$

Then, we can use central, forward or backward differencing at any node.

Central Differencing:

$$\begin{aligned} \alpha_{i,\text{central}}^n &= \left[\frac{2a_i^n}{(z_i - z_{i-1})(z_{i+1} - z_{i-1})} - \frac{b_i^n}{z_{i+1} - z_{i-1}} \right] \\ \beta_{i,\text{central}}^n &= \left[\frac{2a_i^n}{(z_{i+1} - z_i)(z_{i+1} - z_{i-1})} + \frac{b_i^n}{z_{i+1} - z_{i-1}} \right]. \end{aligned} \quad (\text{A.2})$$

Forward/backward Differencing: ($b_i^n > 0$ / $b_i^n < 0$)

$$\begin{aligned} \alpha_{i,\text{forward/backward}}^n &= \left[\frac{2a_i^n}{(z_i - z_{i-1})(z_{i+1} - z_{i-1})} + \max\left(0, \frac{-b_i^n}{z_i - z_{i-1}}\right) \right] \\ \beta_{i,\text{forward/backward}}^n &= \left[\frac{2a_i^n}{(z_{i+1} - z_i)(z_{i+1} - z_{i-1})} + \max\left(0, \frac{b_i^n}{z_{i+1} - z_i}\right) \right]. \end{aligned} \quad (\text{A.3})$$

References

- Barles, G. (1997). Convergence of numerical schemes for degenerate parabolic equations arising in finance. In L. C. G. Rogers and D. Talay (Eds.), *Numerical Methods in Finance*, pp. 1–21. Cambridge University Press, Cambridge.
- Barles, G. and J. Burdeau (1995). The Dirichlet problem for semilinear second-order degenerate elliptic equations and applications to stochastic exit time control problems. *Communications in Partial Differential Equations* 20, 129–178.
- Barles, G., C. Daher, and M. Romano (1995). Convergence of numerical schemes for parabolic equations arising in finance theory. *Mathematical Models and Methods in Applied Sciences* 5, 125–143.

- Barles, G. and E. Jakobsen (2005). Error bounds for monotone approximation schemes for parabolic Hamilton-Jacobi-Bellman equations. Working Paper, Norwegian University of Science and Technology.
- Barles, G. and E. Rouy (1998). A strong comparison result for the Bellman equation arising in stochastic exit time control problems and applications. *Communications in Partial Differential Equations* 23, 1945–2033.
- Barles, G. and P. Souganidis (1991). Convergence of approximation schemes for fully nonlinear equations. *Asymptotic Analysis* 4, 271–283.
- Basak, S. and G. Chabakauri (2007). Dynamic mean-variance asset allocation. Working Paper, London Business School.
- Bielecki, T., J. H. S. Pliska, and X. Zhou (2005). Continuous time mean-variance portfolio selection with bankruptcy prohibition. *Mathematical Finance* 15, 213–244.
- Cairns, A., D. Blake, and K. Dowd (2006). Stochastic lifestyling: optimal dynamic asset allocation for defined contribution pension plans. *Journal of Economic Dynamics and Control* 30, 843–877.
- Chaumont, S. (2004). A strong comparison result for viscosity solutions to Hamilton-Jacobi-Bellman equations with Dirichlet conditions on a non-smooth boundary. Working paper, Institute Elie Cartan, Université Nancy I.
- Chen, Z. and P. Forsyth (2008). A numerical scheme for the impulse control formulation for pricing variable annuities with a guaranteed minimum withdrawal benefit (GMWB). *Numerische Mathematik* 109, 535–569.
- Chiu, M. and D. Li (2006). Asset and liability management under a continuous time mean variance optimization framework. *Insurance: Mathematics and Economics* 39, 330–355.
- Crandall, M. G., H. Ishii, and P. L. Lions (1992). User’s guide to viscosity solutions of second order partial differential equations. *Bulletin of the American Mathematical Society* 27, 1–67.
- Duffie, D. and H. Richardson (1991). Mean variance hedging in continuous time. *Annals of Applied Probability* 1, 1–15.
- Forsyth, P. A. and G. Labahn (2008). Numerical methods for controlled Hamilton-Jacobi-Bellman PDEs in finance. *Journal of Computational Finance* 11 (Winter), 1–44.
- Gerrard, R., S. Haberman, and E. Vigna (2004). Optimal investment choices post retirement in a defined contribution pension scheme. *Insurance: Mathematics and Economics* 35, 321–342.
- Højgaard, B. and E. Vigna (2007). Mean variance portfolio selection and efficient frontier for defined contribution pension schemes. Working Paper, Aalborg University.
- Kahl, C., M. Gunther, and T. Rossberg (2008). Structure preserving stochastic integration schemes in interest rate derivative modelling. *Applied Numerical Mathematics* 58, 284–295.

- Leippold, M., F. Trojani, and P. Vanini (2004). A geometric approach to multiperiod mean variance optimization of assets and liabilities. *Journal of Economic Dynamics and Control* 28, 1079–1113.
- Li, D. and W.-L. Ng (2000). Optimal dynamic portfolio selection: Multiperiod mean variance formulation. *Mathematical Finance* 10, 387–406.
- Li, X. and X. Y. Zhou (2006). Continuous time mean variance efficiency and the 80% rule. *Annals of Applied Probability* 16, 1751–1763.
- Li, X., X. Y. Zhou, and E. B. Lim (2002). Dynamic mean variance portfolio selection with no-shorting constraints. *SIAM Journal on Control and Optimization* 40, 1540–1555.
- Lorenz, J. and R. Almgren (2007). Adaptive arrival price. in *Algorithmic Trading III: Precision, Control, Execution*, Brian R. Bruce, editor, Institutional Investor Journals.
- Merton, R. (1971). Optimum consumption and portfolio rules in a continuous time model. *Journal of Economics Theory* 3, 373–413.
- Nguyen, P. and R. Portrai (2002). Dynamic asset allocation with mean variance preferences and a solvency constraint. *Journal of Economic Dynamics and Control* 26, 11–32.
- Pooley, D., P. Forsyth, and K. Vetzal (2003). Numerical convergence properties of option pricing PDEs with uncertain volatility. *IMA Journal of Numerical Analysis* 23, 241–267.
- Wang, J. and P. Forsyth (2008). Maximal use of central differencing for Hamilton-Jacobi-Bellman PDEs in finance. *SIAM Journal on Numerical Analysis* 46, 1580–1601.
- Wang, Z., J. Xia, and L. Zhang (2007). Optimal investment for the insurer: The martingale approach. *Insurance: Mathematics and Economics* 40, 322–334.
- Zhou, X. and D. Li (2000). Continuous time mean variance portfolio selection: A stochastic LQ framework. *Applied Mathematics and Optimization* 42, 19–33.